

## First Degree in Biochemistry

### Project/Internship Report

Synthesis of a marine-derived analogue with  
potential anti-inflammatory activity and *in silico*  
studies on inhibition of cyclooxygenase enzymes

Ricardo José Faria Pereira

2021

# Synthesis of a marine-derived analogue with potential anti-inflammatory activity and *in silico* studies on inhibition of cyclooxygenase enzymes

**Supervisor:** Professora Doutora Carla Sofia Fernandes

Faculdade de Farmácia da Universidade do Porto / Centro Interdisciplinar de Investigação Marinha e Ambiental (CIIMAR), Universidade do Porto.

**Co-supervisor:** Professora Doutora Maria Elizabeth Tiritan

Faculdade de Farmácia da Universidade do Porto / CESPU – Instituto de Investigação e Formação Avançada em Ciências e Tecnologias da Saúde / Centro Interdisciplinar de Investigação Marinha e Ambiental (CIIMAR), Universidade do Porto.

Laboratório de Química Orgânica e Farmacêutica

Faculdade de Farmácia da Universidade do Porto



Carla Sofia Garcia Fernandes

27-06-2021

This research was supported by national funds by FCT through the projects UIDB/04423/2020 and UIDP/04423/2020 (Group of Natural Products and Medicinal Chemistry - CIIMAR) and ERDF, through the COMPETE – Programa Operacional Fatores de Competitividade (POFC) program in the framework of the program PT2020; the Project No. POCI-01-0145-FEDER-028736, co-financed by COMPETE 2020, under the PORTUGAL 2020 Partnership Agreement, through the ERDF, and CHIRALBIOACTIVE-PI-3RL-IINFACTS-2019 and CHIRALSINTESE-APSFCT-IINFACTS\_2021.



Some results of this work were presented as poster communications:

**Ricardo Pereira**, Joana Teixeira, Maria Elizabeth Tiritan, Carla Fernandes, Madalena Pinto, Synthesis of marine-derived xanthone analogues with potential anti-inflammatory activity, IJUP 2021, 14th Meeting of Young Researchers of University of Porto, Encontro de Investigação Jovem da Universidade do Porto, online, 5-7 May 2021

**Ricardo Pereira**, Joana Teixeira, Maria Elizabeth Tiritan, Carla Fernandes, Madalena Pinto, Marine-derived xanthone analogues with potential anti-inflammatory activity: total synthesis and structure elucidation, VI Jornadas da Bioquímica, online, 7-9 May 2021

## **Acknowledgements**

---

This project was a challenge that I would not be able to overcome without the help of some people.

Firstly, I would like to thank my supervisor, Prof. Dra. Carla Fernandes, and my co-supervisor, Prof. Dra. Maria Elizabeth Tiritan, not only for the scientific orientation, but also for the endless support and kindness that the professors always shown. It was a pleasure to work alongside you.

Secondly, to Dra. Andreia Palmeira for the availability to help in the docking studies, to Dra. Sara Cravo and Gisela Adriano for the knowledge and for the assistance in technical aspects, to Joana Teixeira for the help in the synthetic methodologies, to Rita Lima and Ana Laura for all the help and friendship and to all in the LQOF/CIIMAR research group that always helped and assisted me in the lab.

To my parents and my sister that have always been by my side. Your support and love guided me in these three years.

To my friends Ana, Alex, Dias, Hugo, Maria and Tita. Thank you for changing my life, for the unconditional support and for your strength. These three years would not be the same without you.

## Abstract

---

The xanthone (or 9*H*-xanthen-9-one) derivatives (XDs) are a family of molecules that possess a substantial richness of chemical properties and, consequently, interesting biological and pharmacological activities. The class of xanthenes comprising a carboxylic group, particularly, has seen its role in the field of Medicinal Chemistry becoming increasingly relevant, not only as suitable building blocks for new XDs but in a biological point of view as well.

The Laboratório de Química Orgânica e Farmacêutica/Centro Interdisciplinar de Investigação Marinha e Ambiental (LQOF/CIIMAR) research group has a vast experience in synthesis and biological/pharmacological activity evaluation of XDs. Recently, they have reported the potential anti-inflammatory activity of marine-derived XDs by inhibitory activity of cyclooxygenase enzymes (COX-1 and COX-2). Studies conducted by the same group have also described the evaluation of the anti-inflammatory activity of other marine-derived XDs, specifically carboxylated xanthone derivatives (XCars), based on their capacity to decrease the concentration of the pro-inflammatory cytokine IL-6 on lipopolysaccharide (LPS)-stimulated macrophages. At some concentrations, the compounds led to a higher decrease in the amount of IL-6 than the well-known nonsteroidal anti-inflammatory drugs (NSAIDs).

In this study, the total synthesis of one promising XCar for future screening of the anti-inflammatory activity is described. The synthesis was carried by a multi-step pathway, via diaryl ether intermediate. Its structure elucidation was established by spectroscopic methods (<sup>1</sup>H NMR, <sup>13</sup>C NMR, and IR).

Additionally, molecular docking studies reported a higher binding affinity for the XCars and some of the diaryl ether analogues tested in comparison with well known NSAIDs. A potential selective anti-inflammatory lead-candidate was also reported.

The *in vitro* screening of the anti-inflammatory activity of the synthesized XCar is under development.

**Keywords:** Xanthenes, Carboxylated xanthone derivatives, Diaryl ether intermediate, Chemical synthesis, Molecular docking, Anti-inflammatory activity.

## Resumo

---

Os derivados de xantona (9*H*-xanten-9-ona) são uma família de moléculas que possui uma riqueza substancial de propriedades químicas e, conseqüentemente, de atividades biológicas e farmacológicas interessantes. A classe de xantonas que contém um grupo carboxílico, particularmente, tem visto o seu papel na área da Química Medicinal tornar-se cada vez mais relevante, não só como blocos construtores apropriados para a obtenção de novos derivados xantônicos (DXs), mas também sob o ponto de vista da atividade biológica.

O grupo de investigação do Laboratório de Química Orgânica e Farmacêutica/Centro Interdisciplinar de Investigação Marinha e Ambiental (LQOF/CIIMAR) tem uma vasta experiência em síntese e avaliação da atividade biológica/farmacológica de DXs. Recentemente, reportou a avaliação da atividade anti-inflamatória de DXs, análogos de compostos com origem marinha, através de estudos de inibição das enzimas cicloxigenases (COX-1 e COX-2). Em outros estudos, conduzidos pelo mesmo grupo, foi avaliada a atividade anti-inflamatória de outros DXs, análogos de compostos de origem marinha, especificamente derivados xantônicos carboxilados (XCars), tendo em conta a sua capacidade de diminuir a concentração da citosina pró-inflamatória IL-6 em macrófagos estimulados com lipopolissacarídeos. Em algumas concentrações, os compostos levaram a uma maior diminuição na quantidade de IL-6 quando comparados com fármacos anti-inflamatórios não esteroides conhecidos.

Neste estudo, é descrita a síntese total de um XCar promissor para futura avaliação da atividade anti-inflamatória. A estratégia sintética teve como base a formação de um intermediário éter bifenílico, envolvendo vários passos reacionais. A elucidação estrutural da xantona foi estabelecida por métodos espectroscópicos (<sup>1</sup>H RMN, <sup>13</sup>C RMN, e IV).

Adicionalmente, os estudos de *docking* molecular reportaram uma maior afinidade de ligação para as XCars e alguns análogos de éteres bifenílico em comparação com fármacos anti-inflamatórios não esteroides conhecidos. Um potencial candidato a *lead* anti-inflamatório seletivo foi também reportado.

A avaliação *in vitro* da atividade anti-inflamatória do XCar sintetizado está em desenvolvimento.

**Palavras-chave:** Xantonas, Derivados xantônicos carboxilados, Éter bifenílico, Síntese química, *Docking* molecular, Atividade anti-inflamatória.

## **Abbreviations and Symbols**

---

$^1\text{H}$ NMR	Proton Nuclear Magnetic Resonance
$^{13}\text{C}$ NMR	Carbon Nuclear Magnetic Resonance
$\delta$	Chemical shift
CDX	Chiral derivative of xanthone
COX	Cyclooxygenase
d	Doublet
dd	Double doublet
DMSO- $\text{d}_6$	Hexadeuterodimethyl sulfoxide
GSS	Grover, Shah and Shah reaction
HMBC	Heteronuclear Multiple Bond Correlation
HSQC	Heteronuclear Single Quantum Coherence
IR	Infrared Spectroscopy
LPS	Lipopolysaccharide
NMR	Nuclear Magnetic Resonance
NSAIDs	Nonsteroidal anti-inflammatory drugs
PPA	Polyphosphoric acid
SAR	Structure activity relationship
s	Singlet
TLC	Thin Layer Chromatography
XCar	Carboxylated xanthone derivative

# Index

---

<b>1. Introduction.....</b>	<b>1</b>
1.1.    Xanthone: a privileged structure .....	1
1.2.    Different approaches for the synthesis of xanthenes.....	2
1.3.    Carboxylated xanthone derivatives (XCars) .....	4
1.4.    Aims .....	6
<b>2. Results and Discussion.....</b>	<b>7</b>
2.1.    Chemical Synthesis .....	7
2.1.1.    Synthesis of 6,8-dimethyl-9-oxo-9 <i>H</i> -xanthene-2-carboxylic acid (1, XCar 4).....	7
2.1.2.    Fischer esterification .....	8
2.1.3.    Ullmann condensation.....	9
2.1.4.    Alkaline ester hydrolysis .....	10
2.1.5.    Intramolecular Friedel-Crafts acylation .....	11
2.2.    Structure elucidation .....	13
2.2.1.    Structure elucidation of 6,8-dimethyl-9-oxo-9 <i>H</i> -xanthene-2-carboxylic acid (XCar-4, 1) .....	13
2.3.    Cyclooxygenase inhibition <i>in silico</i> studies .....	14
<b>3. Materials and Methods.....</b>	<b>23</b>
3.1.    General methods.....	23
3.2.    Synthesis of 6,8-dimethyl-9-oxo-9 <i>H</i> -xanthene-2-carboxylic acid (1) .....	23
3.2.1.    Esterification of 4-bromoisophthalic acid (2) to obtain dimethyl 4-bromoisophthalate (3) .....	23
3.2.2.    Ullmann diaryl ether coupling to obtain dimethyl 4-(3,5-dimethylphenoxy) isophthalate (5).....	24
3.2.3.    Hydrolysis of dimethyl 4-(3,5-dimethylphenoxy) isophthalate (5) to obtain 4-(3,5-dimethylphenoxy) isophthalic acid (6) .....	24
3.2.4.    Intramolecular acylation to obtain 6,8-dimethyl-9-oxo-9 <i>H</i> -xanthene-2-carboxylic acid (1) .....	25
3.3.    Computational studies .....	25
3.3.1.    Preparation of Ligands and Macromolecules .....	25
3.3.2.    Docking .....	26
<b>4. Conclusion.....</b>	<b>26</b>
<b>5. References.....</b>	<b>27</b>



## Figure Index

---

<b>Figure 1:</b> Scaffold of the xanthone molecule and numbering.....	1
<b>Figure 2:</b> Resonance forms of the xanthone.....	1
<b>Figure 3:</b> Structure of yicathin C.....	5
<b>Figure 4:</b> <sup>1</sup> H NMR (DMSO-d <sub>6</sub> , 300.13 MHz) and <sup>13</sup> C NMR (DMSO-d <sub>6</sub> , 75.47 MHz) of compound 1.....	14
<b>Figure 5:</b> XCar-P-1,3,8 molecular conformational changes in COX-1 (A) and COX-2 (B) .....	21
<b>Figure 6:</b> (A) COX-2 ribbon representation with XCar1 docked in the COX active site. (B) Docking pose of XCar1 with the residues that establish polar and hydrophobic interactions represented as a surface.....	22

## Table Index

---

<b>Table 1:</b> IR data of 6,8-dimethyl-9-oxo-9 <i>H</i> -xanthene-2-carboxylic acid ( <b>XCar-4, 6</b> ) .....	13
<b>Table 2:</b> Chemical structures of the XCars and diaryl ether derivatives considered in the docking analysis.....	16
<b>Table 3:</b> Docking scores and hydrogen-bond interactions of the molecules under analysis .....	17

## Scheme Index

---

<b>Scheme 1:</b> Resonance forms of the xanthone.....	1
<b>Scheme 2:</b> General approaches for the synthesis of xanthone derivatives.....	3
<b>Scheme 3:</b> Total synthesis of 6,8-dimethyl-9-oxo-9 <i>H</i> -xanthene-2-carboxylic acid (1).....	7
<b>Scheme 4:</b> Synthesis of dimethyl 4-bromoisophthalate (3) .....	8
<b>Scheme 5:</b> Reaction mechanism of the dimethyl 4-bromoisophthalate (3) synthesis. ....	9
<b>Scheme 6:</b> Synthesis of dimethyl 4-(3,5-dimethylphenoxy)isophthalate (5) .....	9
<b>Scheme 7:</b> Oxidative Addition-Reductive Elimination mechanism for the dimethyl 4-(3,5-dimethylphenoxy)isophthalate (5) synthesis, a proposed non-radical reaction mechanism.....	10
<b>Scheme 8:</b> Synthesis of 4-(3,5-dimethylphenoxy)isophthalic acid (6). ....	10
<b>Scheme 9:</b> Reaction mechanism of the 4-(3,5-dimethylphenoxy)isophthalic acid (6) synthesis..	11
<b>Scheme 10:</b> Synthesis of 6,8-dimethyl-9-oxo-9 <i>H</i> -xanthene-2-carboxylic acid (1). ....	11

<b>Scheme 11:</b> Reaction mechanism of the 6,8-dimethyl-9-oxo-9H-xanthene-2-carboxylic acid (XCar4, 1) synthesis. ....	12
---	----

# 1. Introduction

## 1.1. Xanthone: a privileged structure

The xanthone (or *9H*-xanthen-9-one) is an oxygenated heterocyclic molecule with a dibenzo- $\gamma$ -pyrone framework (**Figure 1**). The nucleus of this compound may seem simple, however, it possesses a substantial richness of chemical properties. Firstly, the tricyclic-fused ring system, due to its rigidity, confers stability to the molecule. Furthermore, the resonance forms of the xanthone (**Scheme 1**), provided by the oxygen atoms of the diaryl ether and the carbonyl group, enhance the reactive profile of this compound (Pinto et al., 2021).

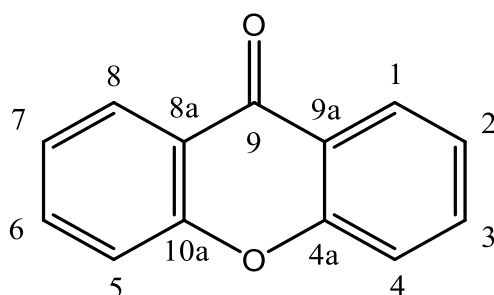
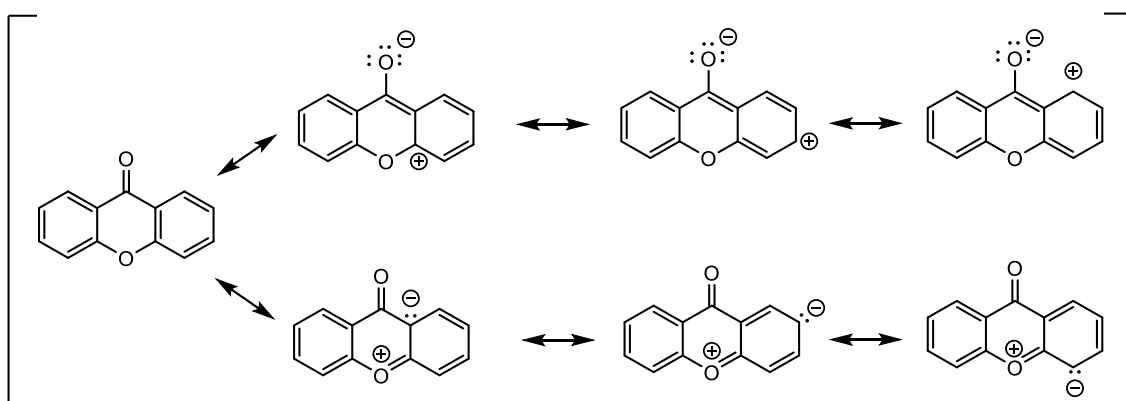


**Figure 1:** Scaffold of the xanthone molecule and numbering.



**Scheme 1:** Resonance forms of the xanthone.

Therefore, the mostly planar and rigid ring system, the carbonyl group at the central ring with the potential for the creation of several interactions, the diaryl ether group favoring the electronic system, as well as the extensive variety of substitution patterns allowed by the xanthone scaffold make this family of compounds reactive to a series of biological targets, resulting in diverse pharmacological activities (Loureiro et

al., 2020; Pinto et al., 2021; Pinto et al., 2005). Thus, the activity of the xanthone nucleus as a pharmacophore, particularly its binding as a high affinity ligand to multiple unrelated classes of protein biotargets, can allow this structure to be considered a privileged scaffold in Medicinal Chemistry (Evans et al., 1988; Pinto et al., 2021).

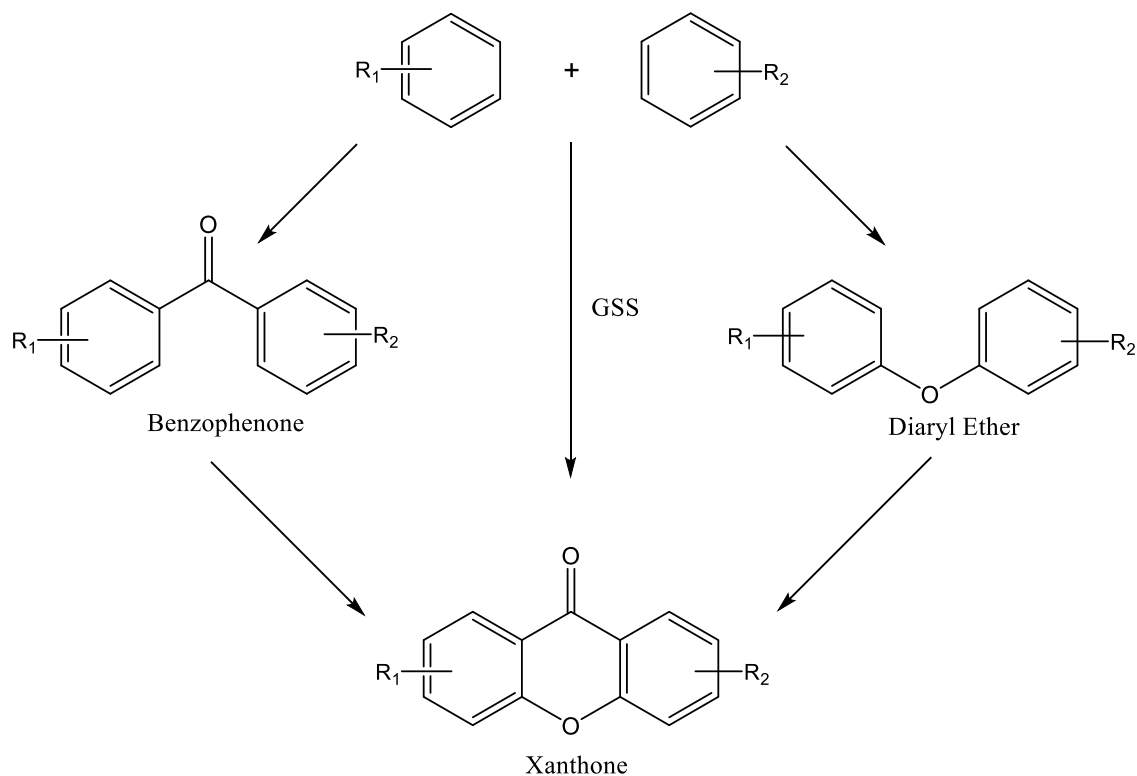
Moreover, most of these compounds exhibit fluorescence, which grants them the possibility to be used in the preparation of fluorescence probes (Sathyadevi et al., 2015; Takashima et al., 2015).

Natural products, as evolutionarily optimized molecules, have always provided inspiration for the process of drug discovery (Shen, 2015). The marine environment, particularly, has been acknowledged as a significant source of unique and rare bioactive substances. Since the oceans are the largest habitat of our planet, a proportionally high biological and chemical diversity should come with no surprise (Lindequist, 2016; Snelgrove, 2016). Marine xanthone derivatives (XDs) have been mainly isolated from fungi and bacteria that either form symbiotic relationships with other micro- and macro-organisms or serve as food to them (Loureiro et al., 2020; Loureiro et al., 2019). This may, as well, explain how compounds similar to these are found as secondary metabolites in marine invertebrates (Pinto et al., 2014).

Nevertheless, these biosynthetic pathways observed in nature create molecules with rather specific substitution patterns and positions throughout the xanthone nucleus. Thus, the total synthesis of these molecules is then necessary for the development of more distinct and diverse compounds that would not be achievable through the molecular modification of natural products. Furthermore, the synthetic methods allow obtaining the compounds in a far greater quantity than what would be possible to obtain from natural products (Azevedo et al., 2012; Loureiro et al., 2020). This also allows, in addition to a biological activity evaluation, structure-activity relationship (SAR) studies of the synthesized xanthenes (Sousa & Pinto, 2005).

## **1.2. Different approaches for the synthesis of xanthenes**

There are three classical methods for the synthesis of simple xanthenes: the Grover, Shah, and Shah (GSS) reaction, the synthesis via benzophenone intermediate and the synthesis via diphenyl ether intermediate (**Scheme 2**) (Azevedo et al., 2012; Sousa & Pinto, 2005).



**Scheme 2:** General approaches for the synthesis of xanthone derivatives.

The GSS method consists in a one-step reaction between a salicylic acid derivative and a suitable phenol. These compounds, heated together while using a strong acid like zinc chloride and phosphoryl chloride as a solvent, allow the formation of the xanthone, assuming that the benzophenone intermediate has a hydroxyl group in either the 6 or 6' position, besides two hydroxyls that must exist in the 2 and 2' positions (Azevedo et al., 2012). Due to these limitations, several multi-step methodologies have been developed.

The benzophenone route is the most common approach for the synthesis of xanthenes, generally affording high yields (Azevedo et al., 2012). While there exist many methods for the formation of the benzophenone intermediate, the Friedel-Crafts acylation is the one commonly used. This electrophilic aromatic substitution between an conveniently substituted benzoyl chloride and a phenolic derivative is usually catalyzed by aluminum chloride and is followed by a cyclization step (Azevedo et al., 2012; Sousa & Pinto, 2005). Nonetheless, the acylation reaction suffers from some drawbacks, considering it lacks regioselectivity and thus the reaction can happen on both *ortho* and *para* positions.

The diaryl ether route with the creation of an ether bond through a copper-catalyzed Ullmann ether synthesis is another strategy for the synthesis of XDs. The

classical coupling of an aryl halide with a phenol derivative, developed by Fritz Ullmann and Irma Goldberg, demanded stoichiometric amounts of copper salts and harsh experimental conditions, such as very high reaction temperatures and long reaction times. The yields obtained were, as well, generally lower compared with the ones described in the other classical routes (Sousa & Pinto, 2005). In the last decade, nevertheless, with the introduction of inexpensive ligands (diamines, aminoalcohols, diketones, diols), this reaction has become truly catalytic, reducing the catalyst loading as low as 1 mol% (Sperotto et al., 2010). By adding these ligands, the solubility of the copper precursors is improved, which allows higher yields for the diaryl ether synthesis under milder reaction conditions (Azevedo et al., 2012). Comparably to what happens in the benzophenone synthetic strategy, a cyclization step follows the synthesis of the intermediate. The modified Ullmann reaction will be explored more extensively in this report.

Overall, these methodologies allow the synthesis of XDs substituted with diverse groups such as hydroxyl, methoxy, methyl, carboxyl, in addition to other more complex substituents (Pinto et al., 2005).

### **1.3. Carboxylated xanthone derivatives (XCars)**

Nowadays, the class of xanthenes substituted with a carboxylic group has seen its role in the field of Medicinal Chemistry becoming more and more relevant (Ribero et al., 2019).

The importance of the carboxylated xanthone derivatives (XCars) takes account the potential that they have as suitable chemical substrates for molecular modifications. This allows the creation of new and more complex xanthenes whose biological activity and SAR can be further studied (Ribero et al., 2019). Such is the case, for example, of the use of XCars as building blocks for the synthesis of chiral derivatives of xanthenes (CDXs). In a practical sense, this can be achieved by coupling a XCar with enantiomerically pure molecules, such as amino alcohols, amino acids, amino esters and amines, using coupling reagents (Carraro et al., 2020; Fernandes et al., 2014; Fernandes, Oliveira, et al., 2012). Furthermore, CDXs, in addition to their attractive biological activities, are also strong candidates for the development of new chiral stationary phases (CSPs) for liquid chromatography (Fernandes et al., 2018; Fernandes, Tiritan, et al., 2012; Fernandes, Tiritan, et al., 2017; Phyo et al., 2020).

Moreover, XCars are valuable for their intrinsic biological activities (Pinto et al., 2005). The most relevant examples in the literature include: antitumoral (Hatami et al., 2020; Shao et al., 2008), as is the case of DMXAA (5,6-dimethyl-9-oxo-9*H*-xanthene-4-acetic acid) which induces apoptosis in tumor vascular endothelial cells (Ching et al., 1999; Ching et al., 2004); antibacterial and antifungal (Liu et al., 2012; Sun et al., 2013); antiallergic (Byars & Ferraresi, 1980; Pfister et al., 1978); among others.

This class of molecules has also shown *in vitro* and *in vivo* anti-inflammatory activity comparable with well-known nonsteroidal anti-inflammatory drugs (NSAIDs) (Librowski et al., 2005; Żelaszczyk et al., 2018). These drugs prevent the synthesis of the arachidonic acid metabolites, prostaglandins and leukotrienes, which are important lipid inflammatory mediators, by inhibiting the activity of the enzymes, cyclooxygenase (COX) and lipoxygenase, respectively. COX-2, particularly, is recognized as the key mediator during inflammatory responses (Feng et al., 2020), being one of the key biotargets for the development of new anti-inflammatory drugs.

As described by Pinto *et col.*, the anti-inflammatory properties of compounds can be evaluated through an assessment of its inhibition of COX-1 and COX-2 enzymes (Fernandes, Palmeira, et al., 2017). In another study by the same group, it was reported the full synthesis of yicathin C (**Figure 2**), a marine natural XCar, among other XDs, which anti-inflammatory activity was then evaluated (Loureiro et al., 2020). The bioassay was established based on the capacity of these molecules to reduce the concentration of the pro-inflammatory cytokine IL-6 (interleukin 6) on lipopolysaccharide (LPS)-stimulated macrophages. The results of this study showed a significant decrease in the amount of IL-6, which could be comparable to the one observed in well-known NSAIDs, namely diclofenac and celecoxib. Overall, these results demonstrate yicathin C has a noteworthy anti-inflammatory activity (Loureiro et al., 2020).

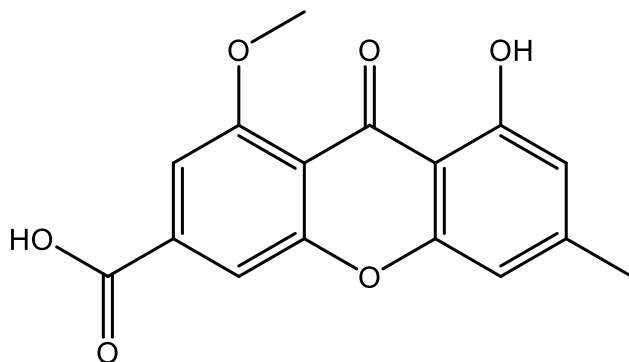


**Figure 2:** Structure of yicathin C.

The discovery of molecules with this kind of properties is particularly important since several NSAIDs exhibit gastric toxicity, a consequence of the direct interactions that these compounds have with the gastric mucosa lipids (Giraud et al., 1999). Studies showed that these compounds interact and disrupt the hydrophobic properties of the outermost lipid layer of the gastric mucosa, increasing its permeability and thus making it more exposed to gastric acid (Hills, 1996). Experimental results suggested, however, that xanthenes have a smaller impact on the bilayer properties of the mucosa, which makes these XCars valuable alternatives for NSAIDs (Markiewicz et al., 2017).

#### 1.4. Aims

One of the main objectives of this project was to synthesize a promising XCar (**Figure 3**), by a multi-step pathway, for further *in vitro* screening of the anti-inflammatory activity. The chosen method to synthesize this compound (**1**) was based on one of the classical methods to obtain XDs, specifically, the diaryl ether route.

The XCar was prepared according to procedures previously established in the research group of LQOF/CIIMAR (Azevedo et al., 2012; Carraro et al., 2020; Fernandes, Oliveira, et al., 2012). The structure elucidation of this molecule was established by spectroscopic methods, such as  $^1\text{H}$  NMR,  $^{13}\text{C}$  NMR and IR.

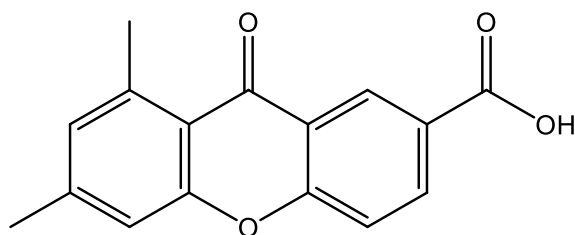


**Figure 3:** Structure of 6,8-dimethyl-9-oxo-9H-xanthene-2-carboxylic acid (**1**)

Computational studies by molecular docking approach were also carried out for a small library of XDs and diaryl ethers, in order to evaluate their affinity to the COX-1 and COX-2 active sites. Additionally, the intermolecular interactions that the ligands and the respective biotargets (enzymes) establish were analyzed.

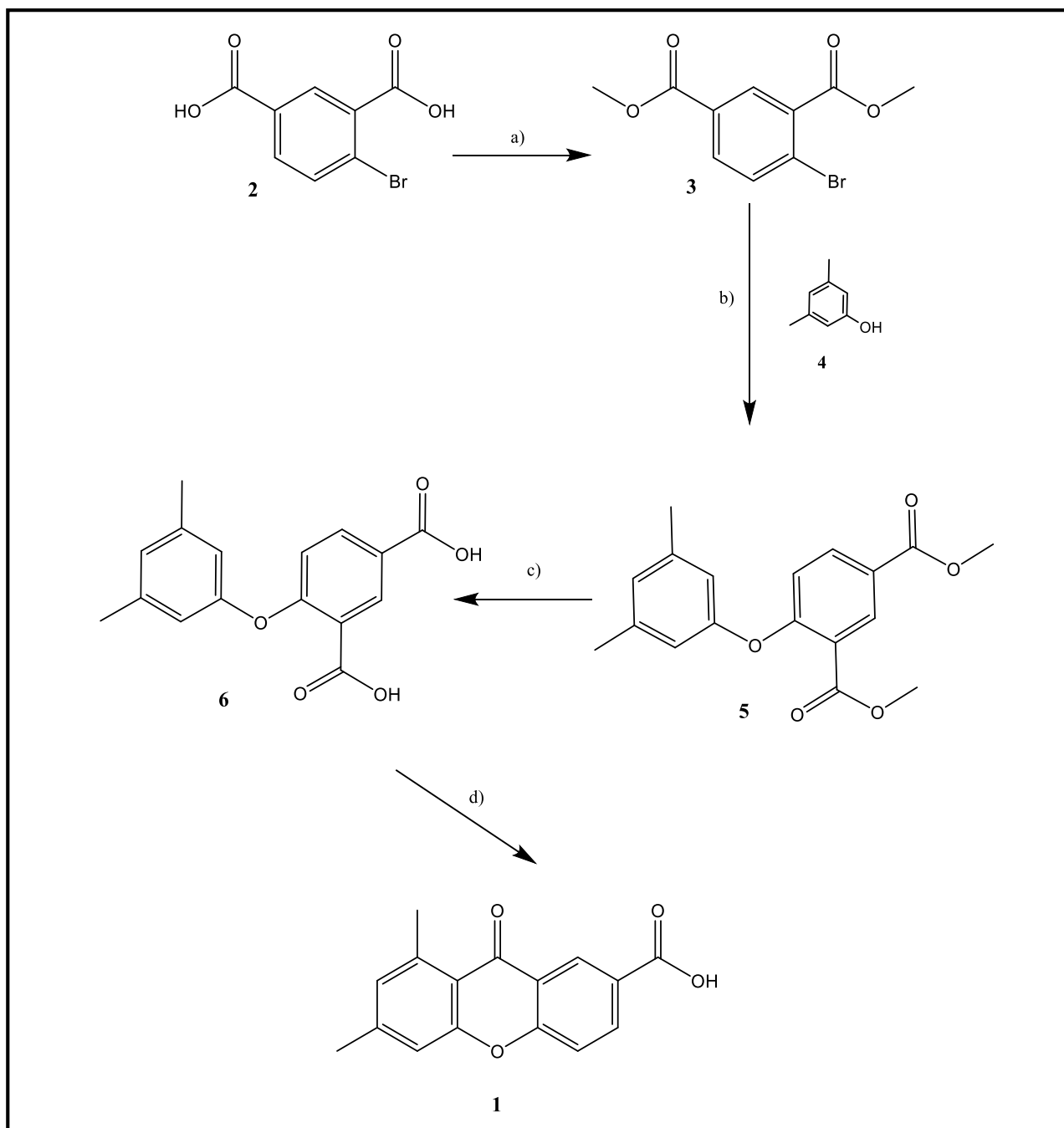


## 2. Results and Discussion

### 2.1. Chemical Synthesis

#### 2.1.1. Synthesis of 6,8-dimethyl-9-oxo-9*H*-xanthene-2-carboxylic acid (**1**, XCar 4)

The multistep-pathway for the synthesis of compound **1** encompasses several chemical reactions as illustrated on **Scheme 3**.



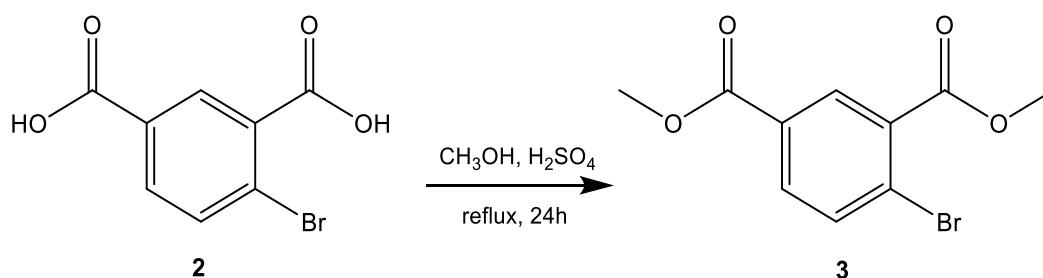
**Scheme 3:** Total synthesis of 6,8-dimethyl-9-oxo-9*H*-xanthene-2-carboxylic acid (**1**).

Reagents and conditions: a) Methanol, H<sub>2</sub>SO<sub>4</sub>, reflux, 24 h; b) CuI, K<sub>3</sub>PO<sub>4</sub>, Picolinic acid, Dioxane, N<sub>2</sub>, 100°C, 48 h; c) Methanol/Tetrahydrofuran (1:1 v/v), 5 M NaOH, room temperature, 24 h; d) Polyphosphoric acid, 80°C, 24 h.

The first step consists in a Fischer esterification (reaction **a**) of the 4-bromoisophthalic acid (**2**), obtaining dimethyl 4-bromoisophthalate (**3**). The Ullmann condensation (reaction **b**) between the aryl bromide **3** and 3,5-dimethylphenol (**4**) took place under a nitrogen atmosphere and a catalytic action of CuI and picolinic acid, resulting in the formation of dimethyl 4-(3,5-dimethylphenoxy)isophthalate (**5**). The diaryl ether **5** was hydrolyzed in alkaline conditions (reaction **c**) to result the 4-(3,5-dimethylphenoxy)isophthalic acid (**6**). The resulting product **6**, through an intramolecular acylation (reaction **d**), afforded 6,8-dimethyl-9-oxo-9*H*-xanthene-2-carboxylic acid (XCar 4, **1**).

### 2.1.2. Fischer esterification

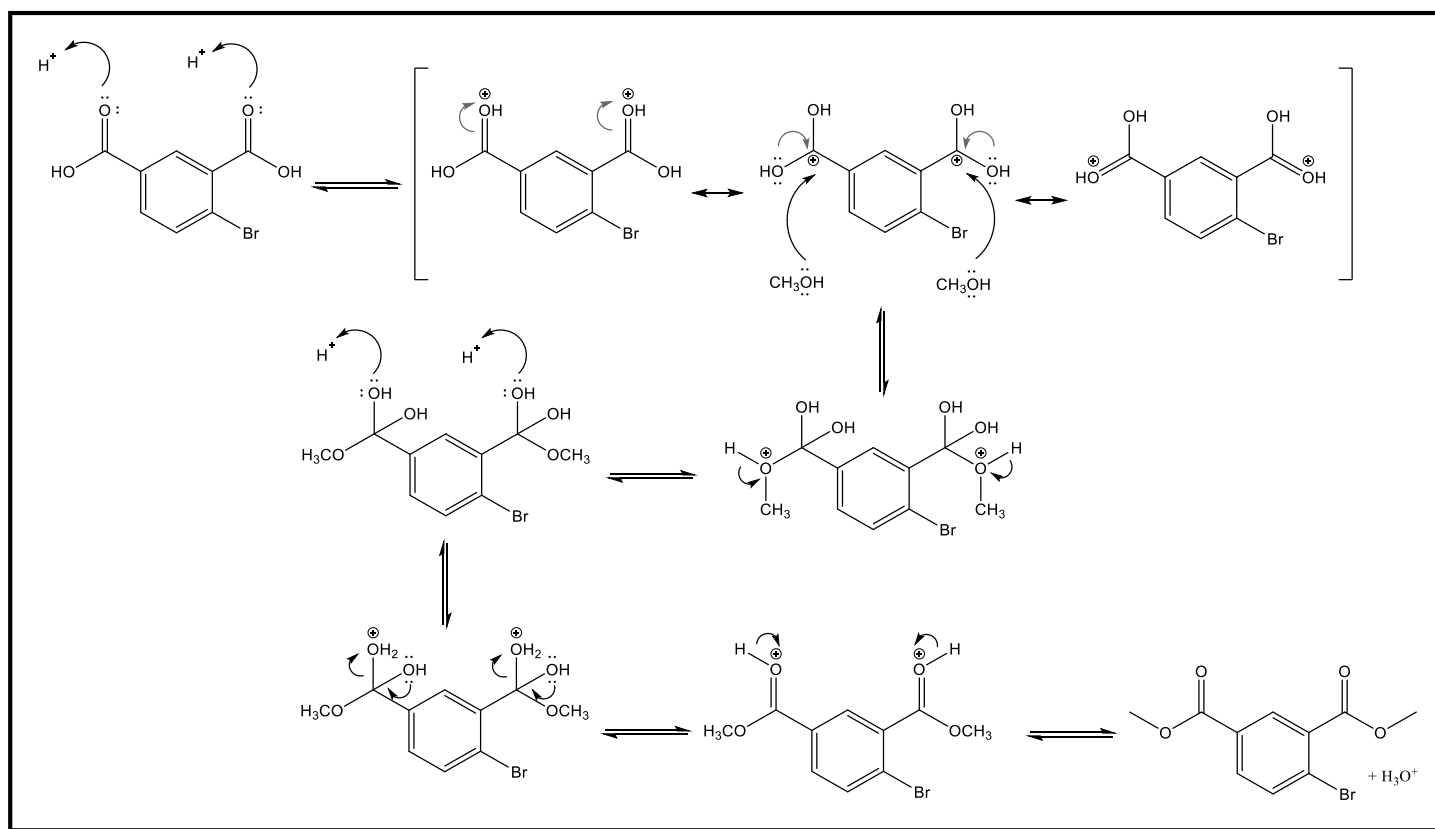
The aryl bromide (**3**) was obtained from the corresponding carboxylic acid (**2**) by Fischer esterification (**Scheme 4**).



**Scheme 4:** Synthesis of dimethyl 4-bromoisophthalate (**3**).

As can be observed in **Scheme 5**, the mechanism for this reaction consists in an acid-catalyzed nucleophilic addition-elimination. The strong inorganic acid, H<sub>2</sub>SO<sub>4</sub>, behaves as a catalyst. Firstly, the protonation of the carbonyl oxygen activated its group towards a nucleophilic attack, which will form the tetrahedral intermediate. Secondly, in the elimination step, the protonation of the hydroxyl group allow the elimination of water, a better leaving group (Vollhardt & Schore, 2003).

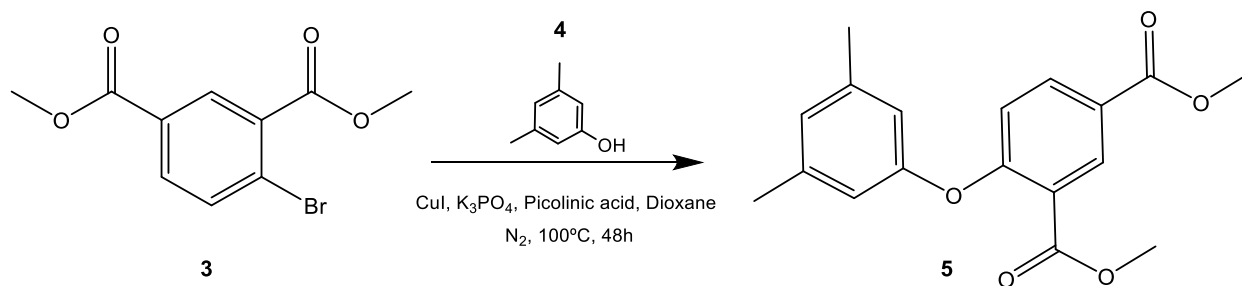
The Fischer esterification is limited by the low-equilibrium constant of all its reversible steps. This is the reason why this reaction is frequently carried out with an excessive amount of one of the two starting materials (Ganeshpure et al., 2007; Yalçinyuva et al., 2008). In this case, the shift of the equilibrium towards the ester formation was accomplished by using methanol as the solvent.



**Scheme 5:** Reaction mechanism of the dimethyl 4-bromoisophthalate (**3**) synthesis.

### 2.1.3. Ullmann condensation

The Ullmann condensation between the aryl bromide **3** with the phenol **4** resulted in the diaryl ether intermediate **5** (Scheme 6).

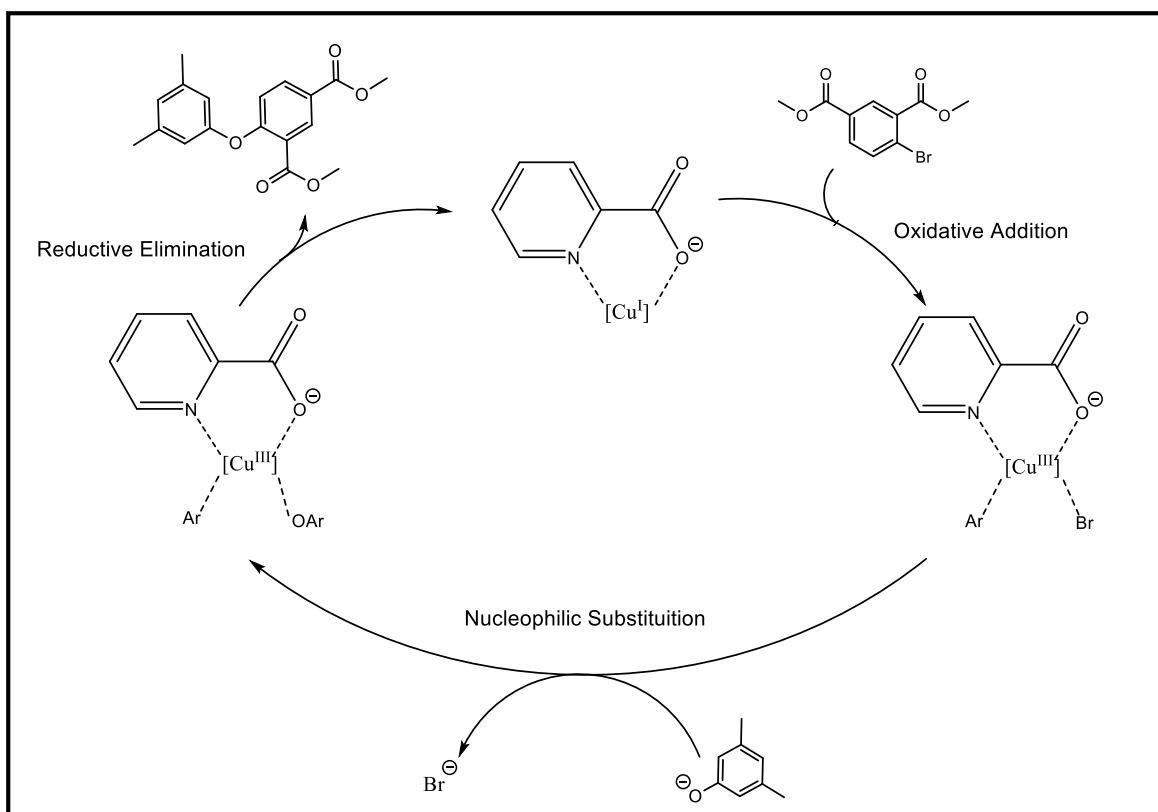


**Scheme 6:** Synthesis of dimethyl 4-(3,5-dimethylphenoxy)isophthalate (**5**).

Although the mechanism for these Cu-assisted *O*-arylation reactions is still unknown, several researchers have proposed theories to explain it (Sperotto et al., 2010; Zhao et al., 2020). One of them is a oxidative addition-reductive elimination mechanism (Scheme 7), which postulates that Cu(I) acts as the active catalytic specie in the reaction (Gurjar & Sharma, 2017). The steps for this mechanism include the oxidative addition of Cu(I) to the aryl halide to form the Cu(III)-intermediate, the nucleophilic substitution by

a phenoxide and the reductive elimination to obtain the diaryl ether and regenerate the Cu(I) catalyst (Zhao et al., 2020).

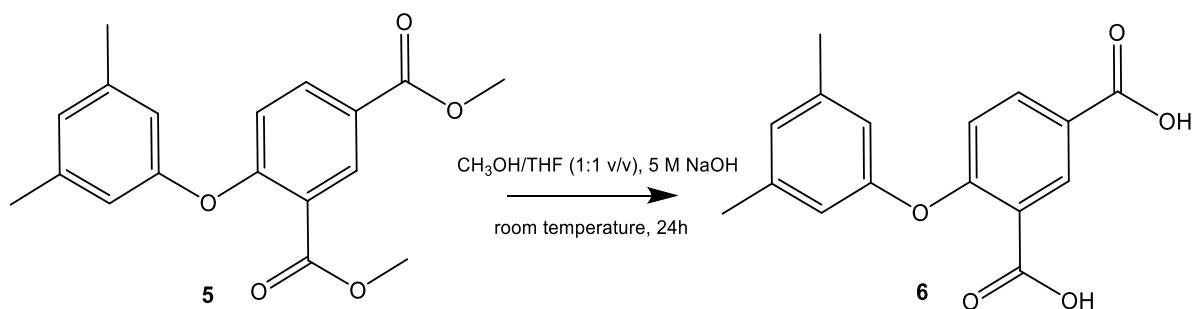
As is the case with the modified Ullmann reactions, bidentate ligands have an indispensable role of enacting the reaction in higher yield and milder conditions. In this case, the compound used was picolinic acid. Additionally, the inorganic base,  $K_3PO_4$ , has a fundamental role in the deprotonation of the nucleophile (Gurjar & Sharma, 2017). The inert atmosphere is also crucial to this reaction, since the presence of oxygen could oxidize and deactivate the catalyst (Altman & Buchwald, 2007).



**Scheme 7:** Oxidative addition-reductive elimination mechanism for the dimethyl 4-(3,5-dimethylphenoxy)isophthalate (**5**) synthesis, a proposed non-radical reaction mechanism (Zhao et al., 2020).

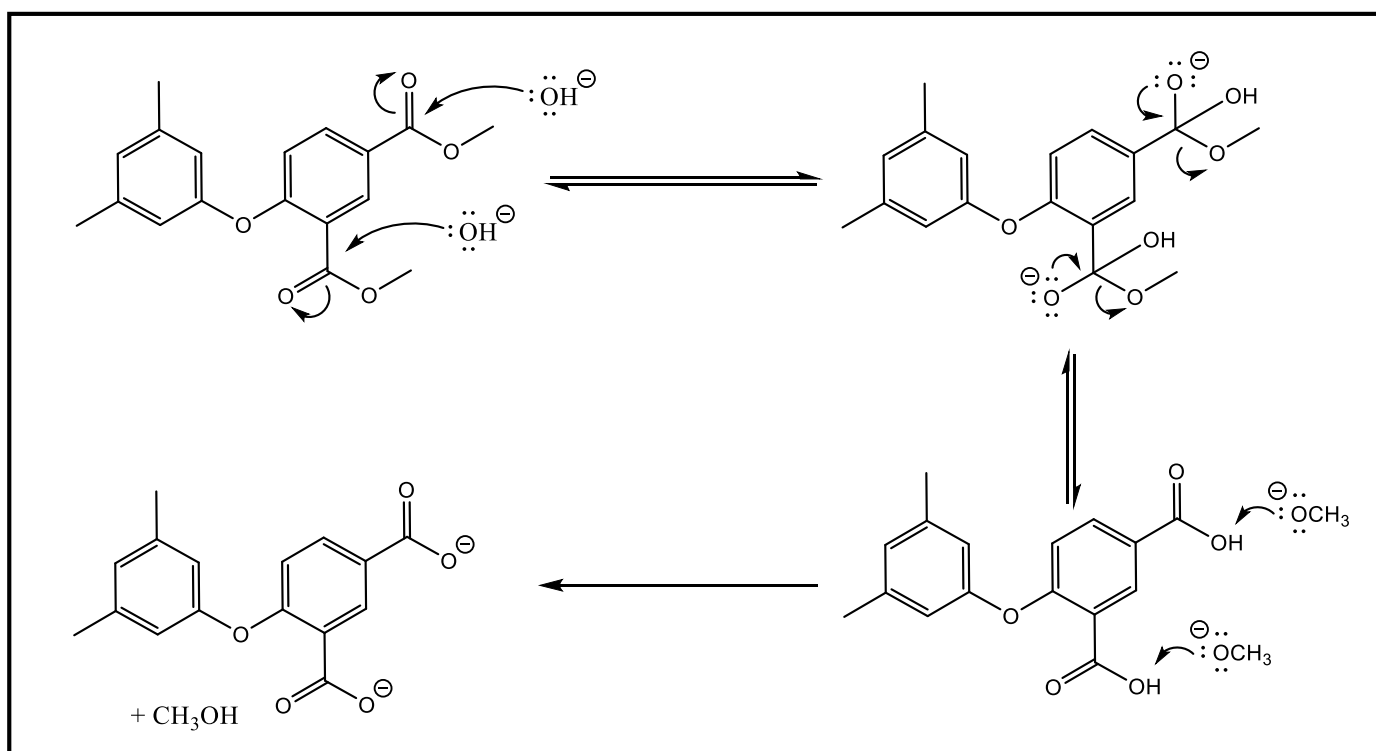
#### 2.1.4. Alkaline ester hydrolysis

The alkaline hydrolysis of the diaryl ether **5** resulted in the corresponding carboxylic acid **6** (Scheme 8).



**Scheme 8:** Synthesis of 4-(3,5-dimethylphenoxy)isophthalic acid (**6**).

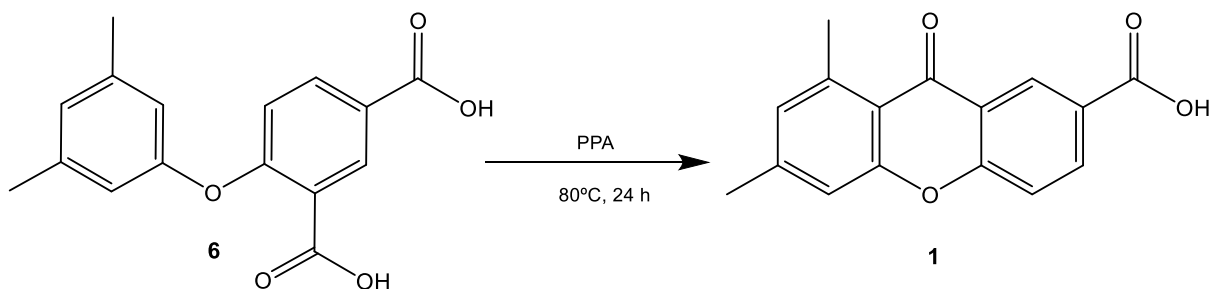
As can be observed in **Scheme 9**, the mechanism for this reaction consists in a base-catalyzed nucleophilic addition-elimination. The hydroxide acts as a nucleophile and attacks the carbonyl group, forming the tetrahedral intermediate. Both hydroxide and methoxide are poor leaving groups; however, the loss of the methoxide group benefits from the very favorable acid-base reaction that occurs in the following step (Vollhardt & Schore, 2003). The carboxylate produced is stabilized by resonance effect, which enables further attacks from the alcohol. The carboxylic acid can be later regenerated through an acidic work-up.



**Scheme 9:** Reaction mechanism of the 4-(3,5-dimethylphenoxy)isophthalic acid (**6**) synthesis.

### 2.1.5. Intramolecular Friedel-Crafts acylation

The intramolecular Friedel-Crafts acylation of 4-(3,5-dimethylphenoxy)isophthalic acid (**6**) afforded the XCar4 (**1**) (**Scheme 10**).

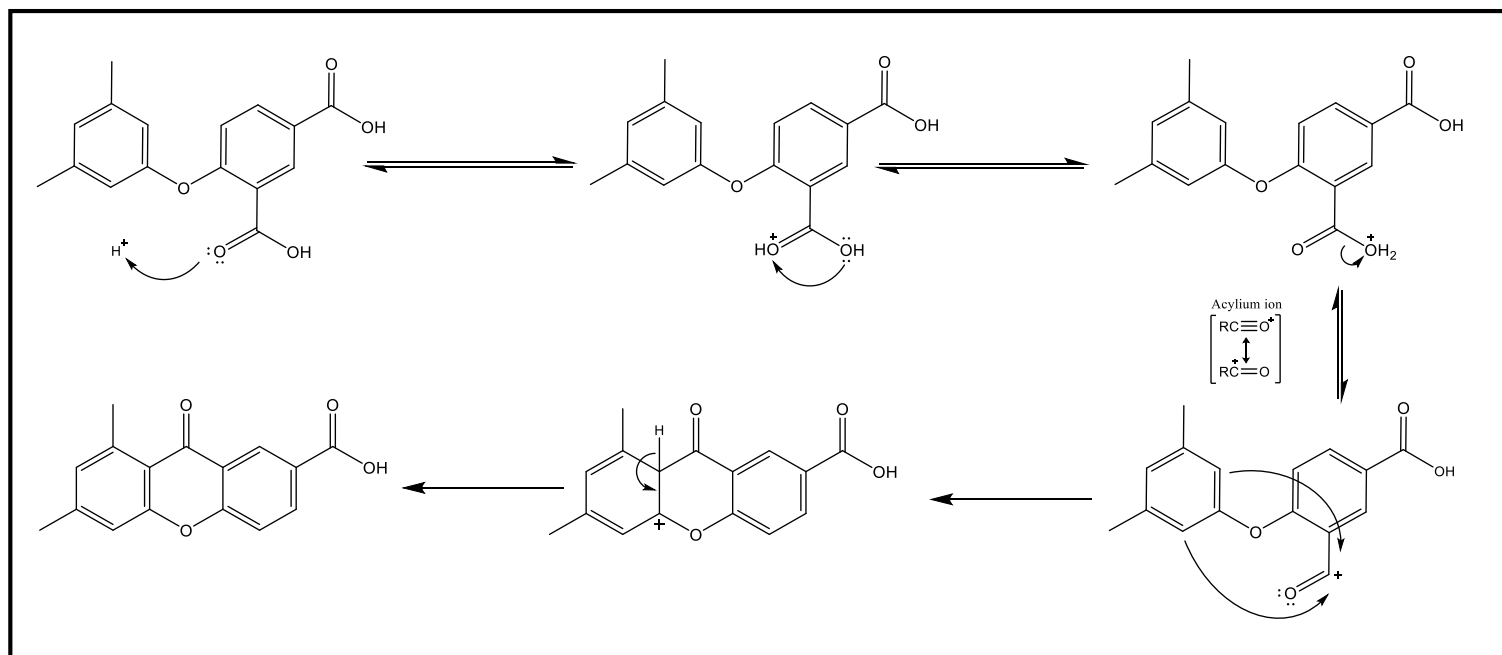


**Scheme 10:** Synthesis of 6,8-dimethyl-9-oxo-9H-xanthene-2-carboxylic acid (**1**).

As demonstrated in **Scheme 11**, the mechanism for this reaction consists in an electrophilic aromatic substitution. Polyphosphoric acid, as a strong protic acid, has the role of the catalyst. It activates the electrophile, producing the resonance-stabilized intermediate, acylium cation. The activated electrophile cation will then be attacked by the aromatic ring building the aromatic ketone and, consequently, the desired xanthone (Vollhardt & Schore, 2003).

The participation of carboxylic acids in Friedel-Crafts acylation reactions is not usual, however, the proximity of the nucleophile to the electrophile in an intramolecular reaction makes it possible.

In this particular case, thanks to the specific chemical structure of the compound **6**, only one XCar was synthesized. Nevertheless, some intramolecular acylations performed to obtain xanthenes, afford two xanthone derivatives that need to be furtherly separated through a flash column chromatography of the corresponding esters of the XDs (Fernandes, Oliveira, et al., 2012).



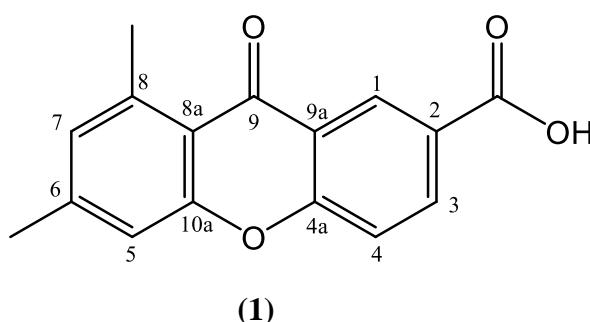
**Scheme 11:** Reaction mechanism of the 6,8-dimethyl-9-oxo-9H-xanthene-2-carboxylic acid (**XCar4, 1**) synthesis.

## 2.2. Structure elucidation

The following IR,  $^1\text{H}$  and  $^{13}\text{C}$  NMR data was used to characterize the XCar derivative. In the case of the intermediates, since they have already been described by the research group, its control was established by TLC (thin layer chromatography) with appropriate mobile phases and standard samples of the expected products.

### 2.2.1. Structure elucidation of 6,8-dimethyl-9-oxo-9*H*-xanthene-2-carboxylic acid (XCar4, **1**)

The 6,8-dimethyl-9-oxo-9*H*-xanthene-2-carboxylic acid (**1**) was obtained through the multi-step pathway described in **Scheme 3**.



The IR spectrum of the compound **1** (**Table 1**) revealed the presence of absorption bands corresponding to the C=O, C-O-C and aromatic C=C bonds associated with the xanthone scaffold, confirming the success of the XCar synthesis and its cyclization step. The two absorption bands corresponding to the Ar-CH<sub>3</sub> (methyl groups) are as well in accordance with the expected results for the synthesized xanthone.

**Table 1:** IR data of 6,8-dimethyl-9-oxo-9*H*-xanthene-2-carboxylic acid (**1**)

Bound	$\nu$ (cm <sup>-1</sup> )
O-H	3600-2700
C=O (ketone)	1701
C=O (carboxylic acid)	1661
C=C (aromatic)	1612, 1456 and 1424
C-O-C (ether)	1278
Ar-CH <sub>3</sub>	768 and 694

The analysis of the  $^1\text{H}$  and  $^{13}\text{C}$  NMR data of compound **1** (**Figure 4**) corroborates the accomplishment of the multi-step pathway, displaying  $\delta$  values consistent with the structure of the XCar.

The  $^1\text{H}$  NMR spectra data revealed signals corresponding to the five aromatic protons of the xanthone nucleus and to the six protons of the two methyl groups.

Concerning the  $^{13}\text{C}$  NMR data, the signal at  $\delta$  177.1 ppm supports the success of the cyclization step, by the formation of a carbonyl group and the formation of the xanthone scaffold. The carbon shifts were assigned with the help of two-dimensional NMR techniques, namely HSQC experiments (for the carbon atoms directly bonded to proton atoms) and HMBC correlations (for the deduction of carbon atoms not directly bonded to proton atoms).

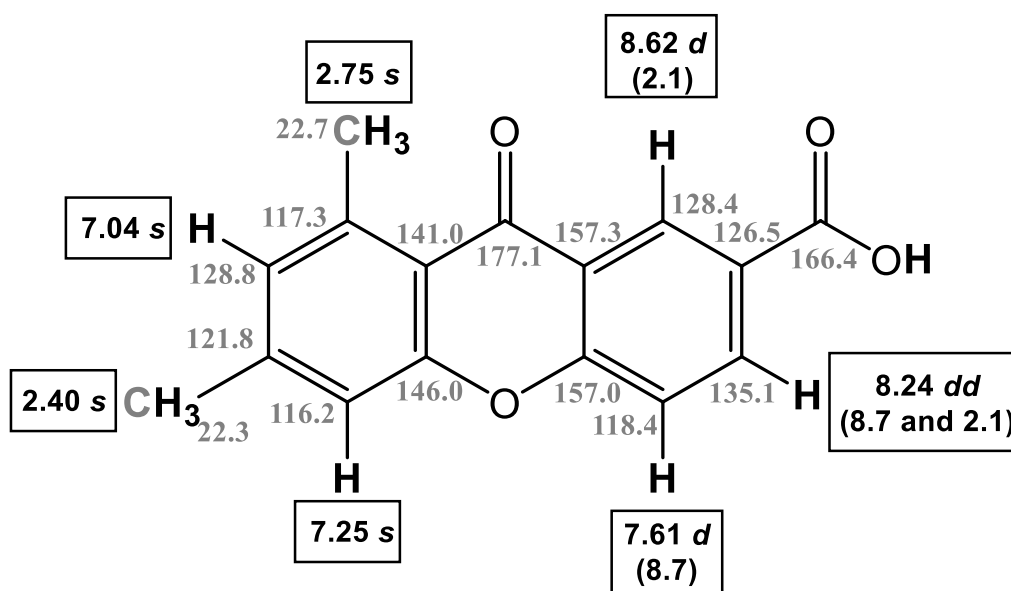


**Figure 4:**  $^1\text{H}$  NMR (DMSO- $d_6$ , 300.13 MHz) and  $^{13}\text{C}$  NMR (DMSO- $d_6$ , 75.47 MHz) of compound **1**.

### 2.3. Cyclooxygenase inhibition *in silico* studies

In order to evaluate the potential anti-inflammatory activity of the synthesized XCar, as well as the activity from other XDs and diaryl ether analogues, molecular docking studies were carried out.

The chosen biotargets for this analysis were the COX-1 and COX-2 enzymes. The cyclooxygenase isoforms are considered noteworthy targets for anti-inflammatory drug development and thus, for its activity studies, due to their role in the synthesis of

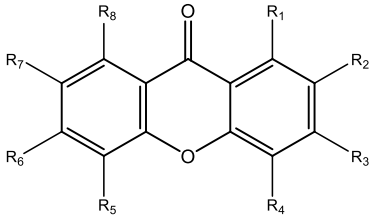
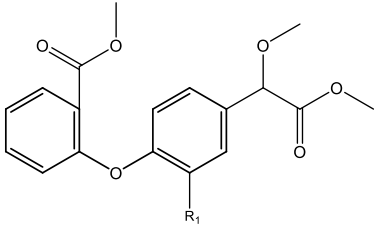
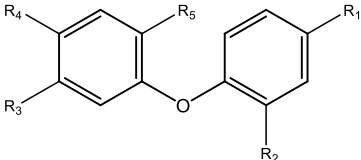


prostaglandins, important inflammatory mediators, and for allowing to inhibit its activity competitively and selectively (Smith et al., 2000). The COX enzymes catalyze the first two steps in prostaglandin synthesis, specifically the oxygenation and reduction reactions that convert the arachidonic acid in prostaglandin H<sub>2</sub> (PGH<sub>2</sub>). This is possible, thanks to the two catalytic sites that these proteins possess. The cyclooxygenase active site catalyzes the first reaction and the peroxidase active site catalyzes the second. Considering this mechanism, most nonsteroidal anti-inflammatory drugs (NSAIDs) were developed as reversible inhibitors of the biosynthesis of prostaglandins by competing with the substrate, the arachidonic acid, for the cyclooxygenase active site (Vane & Botting, 1998).

The two isoforms of the COX enzyme have both functional and structural differences. While COX-1 is constitutively expressed in most tissues and usually has a role in homeostatic functions, such as gastric cytoprotection, the COX-2 isoform is induced and expressed in response to physiological stresses, like infection and inflammation (Rouzer & Marnett, 2009; Smith et al., 2000). Conformational differences have also been discovered between the COX enzymes (Kurumbail et al., 1996). Both enzymes contain the COX active site that consists in a long, hydrophobic channel with the residues Tyr385 and Ser530 at its apex (Vane & Botting, 1998). However, in the COX-2, the substitution of Ile523 with the smaller Val523 creates a secondary internal pocket that branches off from the main channel, allowing the creation of novel and selective interactions. This side-pocket contributes significantly to the larger volume of the cyclooxygenase active site that is found in this isoform (Smith et al., 2000). Traditional NSAIDs can inhibit both COX-1 and COX-2 but generally bind more tightly to COX-1. Consequently, gastrointestinal side-effects may develop in some patients. This led to the development of non-ulcerogenic selective COX-2 inhibitors that exploit the possible interactions with the hydrophilic side-pocket and possess a large volume, which will not allow the drugs to enter the smaller COX-1 active site (Rouzer & Marnett, 2009). Celecoxib and valdecoxib are examples of selective COX-2 inhibitors.

The molecules evaluated in the docking assays are illustrated in **Table 2**.

**Table 2:** Chemical structures of the XCars and diaryl ether derivatives considered in the docking analysis.

	<b>XCar1</b>	$R_3 = \text{OCH}_2\text{COOH}$	$R_1=R_2=R_4=R_5=R_6=R_7=R_8=\text{H}$
	<b>XCar2</b>	$R_6 = \text{OCH}_3 \quad R_2 = \text{COOH}$	$R_1=R_3=R_4=R_7=R_8=\text{H}$
	<b>XCar3</b>	$R_8 = \text{OCH}_3 \quad R_2 = \text{COOH}$	$R_1=R_3=R_4=R_5=R_6=R_7=\text{H}$
	<b>XCar4</b>	$R_6 = R_8 = \text{CH}_3 \quad R_2 = \text{COOH}$	$R_1=R_3=R_4=R_5=R_7=\text{H}$
	<b>XCar5</b>	$R_5 = R_7 = \text{CH}_3 \quad R_2 = \text{COOH}$	$R_1=R_3=R_4=R_6=R_8=\text{H}$
	<b>XCar6</b>	$R_6 = R_7 = \text{CH}_3 \quad R_2 = \text{COOH}$	$R_1=R_3=R_4=R_8=\text{H}$
	<b>XCar7</b>	$R_7 = R_8 = \text{CH}_3 \quad R_2 = \text{COOH}$	$R_1=R_3=R_4=R_5=R_6=R_8=\text{H}$
	<b>XCar-P-1</b>	$R_1 = \text{OCH}_2\text{COOH}$	$R_2=R_3=R_4=R_5=R_6=R_7=R_8=\text{H}$
	<b>XCar-P-1,3</b>	$R_1 = R_3 = \text{OCH}_2\text{COOH}$	$R_2=R_4=R_5=R_6=R_7=R_8=\text{H}$
	<b>XCar-P-1,3,6</b>	$R_1 = R_3 = R_6 = \text{OCH}_2\text{COOH}$	$R_2=R_4=R_5=R_7=R_8=\text{H}$
<hr/>			
	<b>ETM2</b>	$R_1 = \text{H}$	
	<b>ETM3</b>	$R_1 = \text{OCH}_3$	
<hr/>			
	<b>Ester 3</b>	$R_1 = R_2 = \text{COOCH}_3 \quad R_3 = \text{OCH}_3 \quad R_4=R_5=\text{H}$	
	<b>Ester 5</b>	$R_1 = R_2 = \text{CH}_3 \quad R_4 = R_5 = \text{OCH}_3 \quad R_3=\text{H}$	

Known NSAIDs were used as positive controls in this study. Naproxen, piroxicam, diclofenac and indomethacin and (*S*)-ibuprofen are non-selective NSAIDs, while celecoxib and valdecoxib are selective COX-2 inhibitors. Due to its structural similarities with the molecules under analysis, (*S*)-ibuprofen is a particularly interesting positive control.

The docking studies allowed to predict the protein–ligand binding affinity, as well as the ligand conformations and the interactions that they establish with the enzymes. This information was used to evaluate the potential anti-inflammatory activity of the compounds and to identify the residues essential to the COX–ligand binding. The docking scores, the hydrogen interactions established, along with their lengths and the amino acid residues involved, were measured, providing the data shown in **Table 3**.

**Table 3:** Docking scores and hydrogen-bond interactions of the molecules under analysis.

Compounds	Number of H-bonds		Interacting groups		Amino acid residues forming H-bonds (bond length (Å))		Binding energy score (kcal/mol)	
	COX-1	COX-2	COX-1	COX-2	COX-1	COX-2	COX-1	COX-2
Diclofenac	1	0	<u>OH</u> (carboxylic acid)	-	Arg 120 (3.15)	-	-7.1	-8.3
Indomethacin	2	4	<u>O</u> (amide) <u>OH</u> (hydroxyl)	<u>O</u> (carboxylic acid)		His 90 (3.34)	-8.0	-8.3
				<u>OH</u> (carboxylic acid)	Arg 120 (2.86)	Leu 352 (3.07)		
				<u>O</u> (amide)	Leu 352 (2.98)	Tyr 355 (2.61)		
Naproxen	1	2	<u>OH</u> (carboxylic acid)	<u>O</u> (ether)		Arg 120 (3.06)	-8.2	-8.1
				<u>OH</u> (carboxylic acid)	Arg 120 (3.03)	Gly 526 (3.13)		
Piroxicam	3	1	<u>O</u> (amide)		Val 349 (3.16)		-7.1	-8.0
			<u>O</u> (sulfonyl)	<u>O</u> (sulfate)	Ile 523 (2.46)	Ser 530 (2.64)		
			<u>O</u> (sulfonyl)		Ala 527 (2.70)			
Celecoxib	-	4	-	<u>O</u> (sulfonamine)		His 90 (3.18)	-	-10.0
				<u>O</u> (sulfonamine)		His 90 (3.50)		
				<u>N</u> (sulfonamine)		Leu 352 (3.06)		
				<u>O</u> (sulfonamine)		Arg 513 (3.27)		
Valdecoxib	-	2	-	<u>O</u> (sulfonamine)		Tyr 355 (2.90)	-	-9.0
				<u>O</u> (isoxazole)		Tyr 385 (2.71)		
(S)-Ibuprofen	1	0	<u>OH</u> (carboxylic acid)	-	Arg 120 (3.11)	-	-7.7	-7.4
XCar1	1	5	<u>O</u> (carboxylic acid)	<u>OH</u> (carboxylic acid)		His 90 (2.97)	-8.6	-9.4
				<u>O</u> (carboxylic acid)		His 90 (3.24)		
				<u>O</u> (ether)	His 90 (3.14)	Gln 192 (3.00)		
				<u>O</u> (carboxylic acid)		Ser 533 (3.49)		
				<u>O</u> (diaryl ether)		Tyr 355 (2.93)		
XCar2	1	1	<u>O</u> (diaryl ether)	<u>O</u> (carboxylic acid)	Tyr 355 (2.91)	Arg 120 (3.26)	-8.1	-8.4
XCar3	0	1	-	<u>O</u> (diaryl ether)	-	Ser 530 (3.41)	-8.3	-8.6
XCar4	0	1	-	<u>OH</u> (carboxylic acid)	-	Arg 120 (3.26)	-8.4	-9.0

XCar5	1	0	<u>Q</u> (ketone)	-	Ser 530 (2.92)	-	-8.7	-8.5
XCar6	1	0	<u>Q</u> (ketone)	-	Ser 530 (2.86)	-	-8.8	-9.4
XCar7	2	0	<u>Q</u> (carboxylic acid)	-	Tyr 385 (2.92)	-	-8.2	-9.0
			<u>Q</u> (ketone)	-	Ser 530 (2.93)	-	-8.2	-9.0
XCar-P-1	1	0	<u>Q</u> (ketone)	-	Ser 530 (3.20)	-	-8.8	-8.7
XCar-P-1,3	1	5	<u>Q</u> (ketone)	<u>Q</u> (carboxylic acid)	Tyr 355 (3.17)	His 90 (3.10)	-8.6	-8.9
				<u>OH</u> (carboxylic acid)		Gln 192 (2.98)		
				<u>OH</u> (carboxylic acid)		Leu 352 (3.08)		
				<u>Q</u> (ether)		Leu 352 (3.10)		
				<u>Q</u> (carboxylic acid)		Ser 353 (3.37)		
				<u>Q</u> (diaryl ether)		Tyr 355 (3.07)		
XCar-P-1,3,6	1	3	<u>Q</u> (ketone)	<u>Q</u> (ether)	Tyr 355 (3.21)	His 90 (2.73)	-7.4	-8.3
				<u>OH</u> (carboxylic acid) (6)		Leu 352 (2.90)		
				<u>Q</u> (diaryl ether)		Tyr 355 (2.74)		
XCar-P-1,3,8	5	5	<u>OH</u> (carboxylic acid) (1)	<u>Q</u> (carboxylic acid) (1)	His 90 (2.93)	His 90 (3.07)	-6.1	-8.7
			<u>Q</u> (ketone) (3)	<u>Q</u> (ether) (1)	Arg 120 (3.06)	His 90 (3.20)		
			<u>Q</u> (carboxylic acid) (8)	<u>Q</u> (carboxylic acid) (1)	Tyr 385 (2.73)	Gln 192 (2.99)		
			<u>Q</u> (ether) (8)	<u>Q</u> (carboxylic acid) (1)	Tyr 385 (2.80)	Ser 353 (3.47)		
			<u>Q</u> (carboxylic acid) (8)	<u>Q</u> (diaryl ether)	Ser 530 (3.01)	Tyr 355 (2.94)		
ETM2	1	2	<u>Q</u> (ester)	<u>Q</u> (ester)	Arg 120 (3.22)	Arg 120 (3.10)	-6.3	-7.2
				<u>Q</u> (ether)		Tyr 355 (2.67)		
ETM3	2	2	<u>Q</u> (ether)	<u>Q</u> (ester)	Arg 120 (2.81)	Arg 120 (3.10)	-6.1	-7.4
			<u>Q</u> (ether)	<u>Q</u> (ether)	Arg 120 (3.35)	Tyr 355 (2.70)		
Ester 3	1	3	<u>Q</u> (ester)	<u>Q</u> (ester)	Arg 120 (2.77)	His 90 (3.07)	-8.8	-8.9
				<u>Q</u> (ester)		Arg 120 (2.97)		
				<u>Q</u> (ether)		Leu 352 (3.17)		
Ester 5	2	2	<u>Q</u> (ester)	<u>Q</u> (ester)	Arg 120 (2.80)	His 90 (3.33)	-7.6	-9.1
			<u>Q</u> (ester)	<u>Q</u> (ester)	Tyr 355 (3.24)	Arg 120 (2.97)		

Firstly, all the tested compounds successfully docked into the COX-1 and the COX-2 obtaining, with the exception of ETM2 and ETM3, docking scores similar or even more negative to the ones displayed in the positive controls. Arg 120 stands out from all amino acid residues for the way that this residue establishes hydrogen bonds to many ligands in both COX-1 and COX-2 isoforms. Since Arg 120 is one of the few charged amino acids in the COX active site, when the hydrogen acceptor is the OH from a carboxylic acid, this interaction is, more specifically, a salt bridge between the carboxylate anion and the guanidinium cation of the residue (van Ryn et al., 2000). This is the case with the (*S*)-ibuprofen molecule in the COX-1 enzyme and with the XCar2 and XCar4 in COX-2. This interaction is also present in the substrate-enzyme binding mechanism, when Arg 120 binds to the carboxylate group of the arachidonic acid (Smith et al., 2000). Other amino acid residues are also noteworthy in its binding to the ligands non-selectively like Ser 530 and Tyr 355.

Regarding the COX-2 docking results, among the tested molecules, XCar-1 and XCar-6 exhibited the lowest binding free energies which translates in the highest binding affinities. Another ligand that displayed noteworthy results is XCar-P-1,3,8 for achieving a considerable difference between the binding affinities in COX-2 and COX-1. This result is notable in the way that it shows the desirable selectivity that is typical of selective COX-2 inhibitors, thus, with the possibility of avoiding the ulcerogenic pathologies associated with COX-1 inhibition. The synthesized xanthone, XCar4 also exhibited good binding affinity, superior to the one displayed in all positive controls except celecoxib.

While some amino acid residues like His 90 and Gln 192 predominantly establish hydrogen bonds with the tested ligands in the COX-2 enzyme, the discrepancies between the docking scores and the number of H-bonds show that only analyzing the hydrogen interactions is not enough to fully study the network of interactions that these ligands establish with COX-2. This is the case with XCar6, which has the second highest binding affinity in all the tests, while not establishing a single hydrogen interaction. To pursue a deeper understanding of these network, all interactions between the ligands: XCar1, XCar4, XCar6 and celecoxib, were considered and studied as shown in the **Table 4**.

**Table 4:** Comparison of interactions established between COX-2 and some of the test molecules with highest binding affinity. The amino acid residues in bold represent residues exclusive to COX-2.

Celecoxib	XCar1	XCar4	XCar6
His 90	His 90	-	-
Val 116	-	Val 116	Val 116
Arg 120	Arg 120	Arg 120	Arg 120
Gln 192	Gln 192	-	-
Val 349	Val 349	Val 349	Val 349
Leu 352	Leu 352	Leu 352	Leu 352
Ser 353	Ser 353	-	-
Tyr 355	Tyr 355	Tyr 355	Tyr 355
-	-	Leu 359	Leu 359
Phe 381	-	-	-
Tyr 385	-	Tyr 385	Tyr 385
Trp 387	-	Trp 387	Trp 387
<b>Arg 513</b>	<b>Arg 513</b>	-	-
<b>Ala 516</b>	<b>Ala 516</b>	-	-
Ile 517	Ile 517	-	-
Phe 518	Phe 518	Phe 518	Phe 518
-	-	-	Met 522
<b>Val 523</b>	<b>Val 523</b>	<b>Val 523</b>	<b>Val 523</b>
Gly 526	-	-	Gly 526
Ala 527	Ala 527	Ala 527	Ala 527
Ser 530	-	Ser 530	Ser 530
Leu 531	Leu 531	Leu 531	Leu 531

H-bond
  Permanent dipole interaction
  Hydrophobic interaction

The data demonstrates the importance of other types of intermolecular interactions in the ligand-COX-2 binding. Permanent dipole interactions and interactions with the hydrophobic channel stabilize the ligand, increasing its affinity to the binding site (Kurumbail et al., 1996). This, among may help explain how XCar6 has a binding affinity so high without establishing hydrogen interactions.

Among the amino acid residues that interact with the test molecules, Tyr 385 is particularly important since it assumes the role of the catalytic residue and catalyzes the oxygenation reaction. Therefore, binding a ligand to this residue is favorable to the inhibition of the prostaglandin biosynthesis mechanism (Smith et al., 2000). Arg 513, Ala 516 and Val 523, as COX-2 exclusive amino acid residues, have as well a relevant role in the ligand-enzyme binding. For instance, the substitution of His 513 with an arginine residue in the COX-2 isoform, introduce a stable positive charge in the chemical environment of the hydrophobic main chain, enabling selective interactions with polar groups (El-Sayed et al., 2012; Smith et al., 2000). Similarly, Ala 516 (Ser 516 in COX-

1) is another residue that might contribute to specific interactions to the COX-2 enzyme (Kurumbail et al., 1996). The Val 523 amino acid residue, as described earlier, is one of the most important residues in COX-2. By creating the hydrophilic side-pocket and by widening of the hydrophobic channel, this residue leads to conformational changes in the ligands that can heavily impact their binding affinity. This can be observed, comparing the molecular conformation of XCar-P-1,3,8 in COX-1 and COX-2 as illustrated in **Figure 5**.

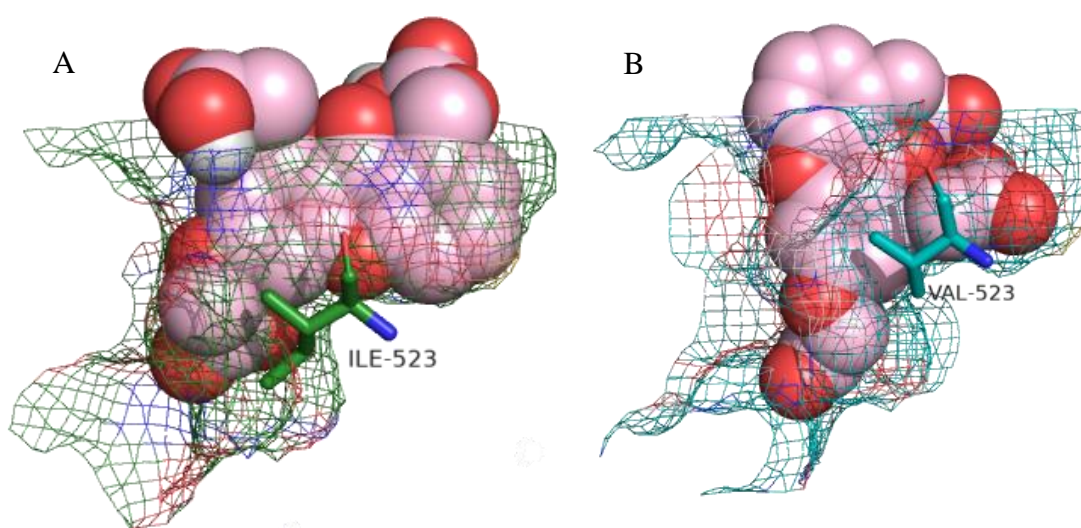


**Figure 5:** XCar-P-1,3,8 molecular conformational changes in COX-1 (A) and COX-2 (B).

To illustrate the results obtained in the docking studies, the representation of XCar1, one of the test molecules with higher binding energy, in the COX-2 active site is represented in **Figure 6**. The hydrogen bonds are illustrated, as well as the surface equivalence of the polar and hydrophobic interactions. Due to the proximity of the aromatic rings of the enzyme residues and the ligand,  $\pi$ - $\pi$  interactions may also be present, further stabilizing the ligand.

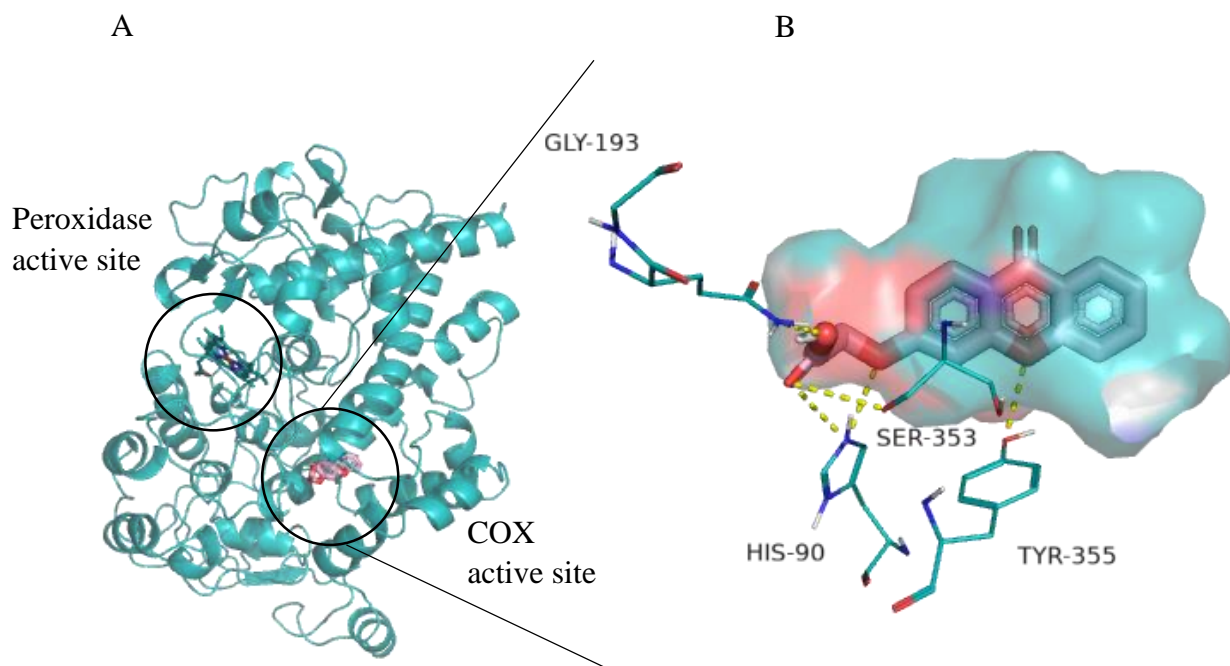


**Figure 6:** (A) COX-2 ribbon representation with XCar1 docked in the COX active site. (B) Docking pose of XCar1 with the residues that establish polar and hydrophobic interactions represented as a surface. The residues represented in lines are the ones who establish hydrogen interactions. These interactions are show as yellow dashes.



### **3. Materials and Methods**

---

#### **3.1. General methods**

All the reactions and purification methodologies were controlled by thin-layer chromatography (TLC) (silica gel, 60 GF<sub>254</sub> Merck) with appropriate mobile phases and UV detection at 245 and 365 nm.

The solvents were evaporated on a rotary evaporator under reduced pressure (rotative evaporator Büchi).

Melting point (m.p.) was determined in a Köfler microscope and are uncorrected.

<sup>1</sup>H and <sup>13</sup>C NMR spectra were performed in the Department of Chemistry of the University of Aveiro, and were taken on Brücker AC-200, DRX-300 or DRX-500 spectrometers (300.13 MHz for <sup>1</sup>H and 75.47 MHz for <sup>13</sup>C), using DMSO-d<sub>6</sub> as solvent. Chemical shifts are expressed in  $\delta$  (ppm) values relative to tetramethylsilane (TMS) used as an internal reference. Coupling constants are expressed in hertz (Hz). <sup>13</sup>C NMR assignments were established by 2D HSQC and HMBC experiments.

IR spectrum was obtained in KBr microplate in a FTIR spectrometer Nicolet iS10 from Thermo Scientific (Waltham, MA, USA) with Smart OMNI-Transmisson accessory (Software 188 OMNIC 8.3).

#### **3.2. Synthesis of 6,8-dimethyl-9-oxo-9H-xanthene-2-carboxylic acid (1)**

##### **3.2.1. Esterification of 4-bromoisophthalic acid (2) to obtain dimethyl 4-bromoisophthalate (3)**

To a solution of 4-bromoisophthalic acid (**2**) (10.00 g, 40.81 mmol) in methanol (600 mL), 7 mL of concentrated H<sub>2</sub>SO<sub>4</sub> was added. Then, the reaction mixture was refluxed for 24 h. After evaporation of the methanol, water (100 mL) was added and the crude product was extracted with diethyl ether (3 x 100 mL). The organic layer was washed with water (100 mL), saturated NaHCO<sub>3</sub> solution (3 x 120 mL) and water (2 x 100 mL), successively. After drying with anhydrous sodium sulfate and filtered, the solvent was evaporated under reduced pressure affording a white solid. The TLC analysis, using a standard sample of compound **3** (previously synthesized by the LQOF/CIIMAR research group), lead to the conclusion that the product obtained was dimethyl 4-bromoisophthalate (**3**). Yield: 84%.

### 3.2.2. Ullmann diaryl ether coupling to obtain dimethyl 4-(3,5-dimethylphenoxy) isophthalate (**5**)

A mixture of dimethyl 4-bromoisophthalate (**3**) (3.00 g, 10.99 mmol), 3,5-dimethylphenol (**4**) (2.10 g, 17.19 mmol), CuI (0.32 g, 1.68 mmol), K<sub>3</sub>PO<sub>4</sub> (7.23 g, 34.06 mmol) and picolinic acid (0.63 g, 5.11 mmol) was transferred to a sealed flask, which it was then evacuated and backfilled with nitrogen. The evacuation/backfill sequence was repeated two additional times. Dry dioxane (27 mL) was added under nitrogen atmosphere. The sealed flask was placed in a preheated oil bath (100°C) and the reaction mixture was stirred vigorously with a magnetic stirrer for 48 h. The reaction mixture was cooled to room temperature. After evaporation of the organic solvent, water (50 mL) was added and the crude product was extracted with diethyl ether (3 x 50 mL). The organic layer was washed with water (2 x 50 mL), saturated CuSO<sub>4</sub> solution (2 x 50 mL) and 0.1 M NaOH solution (2 x 50 mL). After drying with anhydrous sodium sulfate and filtered, the solvent was evaporated under reduced pressure providing an oily dark product. The TLC analysis, using a standard sample of compound **5** (previously synthesized by the LQOF/CIIMAR research group), lead to the conclusion that the product obtained was dimethyl 4-(3,5-dimethylphenoxy) isophthalate (**5**). Yield: 30%

### 3.2.3. Hydrolysis of dimethyl 4-(3,5-dimethylphenoxy) isophthalate (**5**) to obtain 4-(3,5-dimethylphenoxy) isophthalic acid (**6**)

Dimethyl 4-(3,5-dimethylphenoxy) isophthalate (**5**) (1.04 g, 3.30 mmol) was dissolved in methanol/tetrahydrofuran (1:1 v/v) and stirred at room temperature with 5 M NaOH solution (12 mL) for 24 h. After evaporation of the organic solvents, water was added (50 mL) and the crude product was washed with dichloromethane (2 x 100 mL). The organic layer was extracted with water (2 x 50 mL). The aqueous layer was acidified with 5 M HCl solution and extracted with ethyl acetate (2 x 50 mL). The resulting organic layer was dried with anhydrous sodium sulfate, filtered and evaporated under reduced pressure providing a brown solid. The TLC analysis, using a standard sample of compound **6** (previously synthesized by the LQOF/CIIMAR research group), lead to the conclusion that the product obtained was dimethyl 4-(3,5-dimethylphenoxy) isophthalic acid (**6**). Yield: 60%

### 3.2.4. Intramolecular acylation to obtain 6,8-dimethyl-9-oxo-9*H*-xanthene-2-carboxylic acid (**1**)

A solution of 4-(3,5-dimethylphenoxy) isophthalic acid (**6**) (0.50 g, 1.75 mmol) in polyphosphoric acid (3.50 mL) was heated up to 80°C and stirred for 24 h. The reaction mixture was poured over ice, resulting in the formation of a dark brown solid that was collected by filtration under reduced pressure and dried at room temperature to provide 6,8-dimethyl-9-oxo-9*H*-xanthene-2-carboxylic acid (**XCar-4, 1**). Yield: 52%; m.p. >300 °C; IR  $\nu_{\max}$  (cm<sup>-1</sup>) (KBr): 3000-2800, 1661, 1612, 1456, 1424, 1278, 768, 694; <sup>1</sup>H NMR (DMSO-d<sub>6</sub>, 300.13 MHz)  $\delta$ : 8.62 (1H, d, J= 2.1 Hz, H-1), 8.24 (1H, dd, J= 8.7 and 2.1 Hz, H-3), 7.61 (1H, d, J= 8.7 Hz, H-4), 7.25 (1H, s, H-8), 7.04 (1H, s, H-6), 2.75 (3H, s, C-7-CH<sub>3</sub>), 2.40 (3H, s, C-5-CH<sub>3</sub>); <sup>13</sup>C NMR (DMSO, 75.47 MHz)  $\delta$ : 177.1 (C-9), 166.4 (C=OOH), 157.3 (C-9a), 157.0 (C-4a), 146.0 (C-10a), 141.0 (C-8a), 135.1 (C-3), 128.8 (C-7), 128.4 (C-1), 126.5 (C-2), 121.8 (C-6), 118.4 (C-4), 117.3 (C-8), 116.2 (C-5), 22.7 (C-6-CH<sub>3</sub>), 22.3 (C-8-CH<sub>3</sub>).

### 3.3. Computational studies

#### 3.3.1. Preparation of Ligands and Macromolecules

The 2D structure of the small molecules was drawn using ChemDraw v20.0 (PerkinElmer Informatics, Waltham, MA, USA). The ChemBio3D v20.0 software was utilized to obtain the 3D structure of the compounds. A molecular mechanics (MM2) energy minimization was furtherly performed to identify the most stable and least energetic molecule conformation.

The protein coordinates of the COX-1 and COX-2 X-ray crystal structures (PDB codes 3n8x and 1cx2, respectively) were downloaded from Protein Data Bank of Brookhaven.

All structures were prepared and optimized for the docking analysis using AutoDockTools (ADT) v1.5.6 (Molecular Graphics Lab, La Jolla, CA, USA), which corrects the partial charges of both the small molecules and the target enzymes, as well as performs other chemical modifications needed for the success of the following analysis.

### 3.3.2. Docking

The docking studies between the ligands (XDs, diaryl ethers and positive controls) and the enzymes were carried out with the AutoDock Vina software embedded in PyRx-Virtual Screening Tool (Molecular Graphics Lab, La Jolla, CA, USA). The software considered a fixed conformation of the enzyme units, while allowing ligands to be flexible and adapt to the binding site of the respective biotarget. Vina identified potential docking poses for the ligands, from which the ones with the highest binding affinity conformations were chosen. The software was run with an exhaustiveness of 8 and a grid box with the dimensions of X: 21.6, Y: 22.3, Z: 20.2 for COX-1; X: 22.9, Y: 23.7, Z: 21.7 for COX-2.

The visual inspection and graphical representation of the docking results were established with Pymol v2.3.4 (Schrödinger, New York, NY, USA), as well as the identification of the hydrogen bonds, bond lengths and other interactions between the enzymes and all the ligands.

## 4. Conclusion

---

In this project the total synthesis of 6,8-dimethyl-9-oxo-9*H*-xanthene-2-carboxylic acid (**XCar4**) was reported. The synthesis was accomplished by a multi-step synthetic pathway, via diaryl ether intermediate. The success of this pathway was verified by structure elucidation methods, namely IR, <sup>1</sup>H and <sup>13</sup>C NMR. The evaluation of the *in vitro* anti-inflammatory activity of the obtained XCar is under investigation.

In the molecular docking assays of a small library of XDs and diaryl ether analogues, all the XCars and two of the diaryl ethers displayed higher binding affinity than well known NSAIDs. Moreover, XCar-P-1,3,8 exhibited a significative selective binding to COX-2, which gives this compound the potential to be furtherly explored as a novel non-ulcerogenic anti-inflammatory lead-candidate.

## 5. References

---

- Altman, R. A., & Buchwald, S. L. (2007). Cu-catalyzed Goldberg and Ullmann reactions of aryl halides using chelating N- and O-based ligands. *Nature Protocols*, 2(10), 2474-2479.
- Azevedo, C. M. G., Afonso, C. M. M., & Pinto, M. M. M. (2012). Routes to Xanthoness: An Update on the Synthetic Approaches. *Curr. Org. Chem.*, 16.
- Byars, N. E., & Ferraresi, R. W. (1980). Inhibition of rat intestinal anaphylaxis by various anti-inflammatory agents. *Agents and Actions*, 10(3), 252-257.
- Carraro, M. L., Marques, S., Silva, A. S., Freitas, B., Silva, P. M. A., Pedrosa, J., De Marco, P., Bousbaa, H., Fernandes, C., Tiritan, M. E., Silva, A. M. S., & Pinto, M. M. M. (2020). Synthesis of New Chiral Derivatives of Xanthoness with Enantioselective Effect on Tumor Cell Growth and DNA Crosslinking. *ChemistrySelect*, 5(33), 10285-10291.
- Ching, L.-M., Goldsmith, D., Joseph, W. R., Körner, H., Sedgwick, J. D., & Baguley, B. C. (1999). Induction of Intratumoral Tumor Necrosis Factor (TNF) Synthesis and Hemorrhagic Necrosis by 5,6-Dimethylxanthenone-4-Acetic Acid (DMXAA) in TNF Knockout Mice. *Cancer Res.*, 59(14), 3304-3307.
- Ching, L.-M., Zwain, S., & Baguley, B. C. (2004). Relationship between tumour endothelial cell apoptosis and tumour blood flow shutdown following treatment with the antivascular agent DMXAA in mice. *Br. J. Cancer*, 90(4), 906-910.
- El-Sayed, M. A. A., Abdel-Aziz, N. I., Abdel-Aziz, A. A. M., El-Azab, A. S., & ElTahir, K. E. H. (2012). Synthesis, biological evaluation and molecular modeling study of pyrazole and pyrazoline derivatives as selective COX-2 inhibitors and anti-inflammatory agents. Part 2. *Biorg. Med. Chem.*, 20(10), 3306-3316.
- Evans, B. E., Rittle, K. E., Bock, M. G., DiPardo, R. M., Freidinger, R. M., Whitter, W. L., Lundell, G. F., Veber, D. F., Anderson, P. S., Chang, R. S. L., Lotti, V. J., Cerino, D. J., Chen, T. B., P. J. Kling, Kunkel, K. A., Springer, J. P., & Hirshfield, J. (1988). Methods for Drug Discovery: Development of Potent, Selective, Orally Effective Cholecystokinin Antagonists. *J. Med. Chem.*, 31, 2235-2246.
- Feng, Z., Lu, X., Gan, L., Zhang, Q., & Lin, L. (2020). Xanthoness, A Promising Anti-Inflammatory Scaffold: Structure, Activity, and Drug Likeness Analysis. *Molecules*, 25(3), 598.
- Fernandes, C., Masawang, K., Tiritan, M. E., Sousa, E., de Lima, V., Afonso, C., & Pinto, M. M. (2014). New chiral derivatives of xanthoness: Synthesis and investigation of enantioselectivity as inhibitors of growth of human tumor cell lines. *Biorg. Med. Chem.*, 22(3), 1049-1062. .
- Fernandes, C., Oliveira, L., Tiritan, M. E., Leitao, L., Pozzi, A., Noronha-Matos, J. B., Correia-de-Sá, P., & Pinto, M. M. (2012). Synthesis of new chiral xanthone derivatives acting as nerve conduction blockers in the rat sciatic nerve. *European Journal of Medicinal Chemistry*, 55, 1-11.
- Fernandes, C., Palmeira, A., Ramos, I., Carneiro, C., Afonso, C., Tiritan, M. E., Cidade, H., Pinto, P., Saraiva, M., Reis, S., & Pinto, M. (2017). Chiral Derivatives of Xanthoness: Investigation of the Effect of Enantioselectivity on Inhibition of Cyclooxygenases

- (COX-1 and COX-2) and Binding Interaction with Human Serum Albumin. *Pharmaceuticals*, 10(4), 50.
- Fernandes, C., Phyo, Y. Z., Silva, A. S., Tiritan, M. E., Kijjoa, A., & Pinto, M. M. M. (2018). Chiral Stationary Phases Based on Small Molecules: An Update of the Last 17 Years. *Separation & Purification Reviews*, 47(2), 89-123.
- Fernandes, C., Tiritan, M. E., Cass, Q., Kairys, V., Fernandes, M. X., & Pinto, M. (2012). Enantioseparation and chiral recognition mechanism of new chiral derivatives of xanthenes on macrocyclic antibiotic stationary phases [Article]. *Journal of Chromatography A*, 1241, 60-68.
- Fernandes, C., Tiritan, M. E., Cravo, S., Phyo, Y. Z., Kijjoa, A., Silva, A. M. S., Cass, Q. B., & Pinto, M. M. M. (2017). New chiral stationary phases based on xanthone derivatives for liquid chromatography. *Chirality*, 29(8), 430-442.
- Ganeshpure, P. A., George, G., & Das, J. (2007). Application of triethylammonium salts as ionic liquid catalyst and medium for Fischer esterification. *Arkivoc*, 2007(8), 273-278.
- Giraud, M.-N., Motta, C., Romero, J. J., Bommelaer, G., & Lichtenberger, L. M. (1999). Interaction of indomethacin and naproxen with gastric surface-active phospholipids: a possible mechanism for the gastric toxicity of nonsteroidal anti-inflammatory drugs (NSAIDs)\*\*Prof. J. Delattre, personal communication. *Biochem. Pharmacol.*, 57(3), 247-254.
- Gurjar, K. K., & Sharma, R. K. (2017). Mechanistic Studies of Ullmann-Type C–N Coupling Reactions: Carbonate-Ligated Copper(III) Intermediates [Article]. *ChemCatChem*, 9(5), 862-869.
- Hatami, E., Nagesh, P. K. B., Jaggi, M., Chauhan, S. C., & Yallapu, M. M. (2020). Gambogic acid potentiates gemcitabine induced anticancer activity in non-small cell lung cancer [Article]. *Eur. J. Pharmacol.*, 888, Article 173486.
- Hills, B. A. (1996). Gastric surfactant and the hydrophobic mucosal barrier. *Gut*, 39(5), 621-624.
- Kurumbail, R. G., Stevens, A. M., Gierse, J. K., McDonald, J. J., Stegeman, R. A., Pak, J. Y., Gildehaus, D., Iyashiro, J. M., Penning, T. D., Seibert, K., Isakson, P. C., & Stallings, W. C. (1996). Structural basis for selective inhibition of cyclooxygenase-2 by anti-inflammatory agents. *Nature*, 384(6610), 644-648.
- Librowski, T., Czarnecki, R., Czekaj, T., & Marona, H. (2005). New xanthone derivatives as potent anti-inflammatory agents. *Medicina (Kaunas)*, 41, 54–58.
- Lindequist, U. (2016). Marine-Derived Pharmaceuticals - Challenges and Opportunities. *Biomolecules & Therapeutics*, 24(6), 561-571.
- Liu, L.-L., Xu, Y., Han, Z., Li, Y.-X., Lu, L., Lai, P.-Y., Zhong, J.-L., Guo, X.-R., Zhang, X.-X., & Qian, P.-Y. (2012). Four New Antibacterial Xanthenes from the Marine-Derived Actinomycetes *Streptomyces caelestis*. *Mar. Drugs*, 10(12), 2571-2583.
- Loureiro, D. R. P., Magalhães, Á. F., Soares, J. X., Pinto, J., Azevedo, C. M. G., Vieira, S., Henriques, A., Ferreira, H., Neves, N., Bousbaa, H., Reis, S., Afonso, C. M. M., & Pinto, M. M. M. (2020). Yicathins B and C and Analogues: Total Synthesis, Lipophilicity and Biological Activities. *ChemMedChem*, 15(9), 749-755.

- Loureiro, D. R. P., Soares, J. X., Costa, J. C., Magalhães, Á. F., Azevedo, C. M. G., Pinto, M. M. M., & Afonso, C. M. M. (2019). Structures, Activities and Drug-Likeness of Anti-Infective Xanthone Derivatives Isolated from the Marine Environment: A Review. *Molecules*, 24(2), 243.
- Markiewicz, M., Librowski, T., Lipkowska, A., Serda, P., Baczynski, K., & Pasenkiewicz-Gierula, M. (2017). Assessing gastric toxicity of xanthone derivatives of anti-inflammatory activity using simulation and experimental approaches. *Biophys. Chem.*, 220, 20-33.
- Pfister, J. R., Ferraresi, R. W., Harrison, I. T., Rooks, W. H., & Fried, J. H. (1978). Synthesis and antiallergic activity of some mono- and disubstituted xanthone-2-carboxylic acids. *J. Med. Chem.*, 21(7), 669-672.
- Phyo, Y. Z., Teixeira, J., Tiritan, M. E., Cravo, S., Palmeira, A., Gales, L., Silva, A. M. S., Pinto, M. M. M., Kijjoa, A., & Fernandes, C. (2020). New chiral stationary phases for liquid chromatography based on small molecules: Development, enantioresolution evaluation and chiral recognition mechanisms. *Chirality*, 32(1), 81-97.
- Pinto, M. M. M., Castanheiro, R. A. P., & Kijjoa, A. (2014). Xanthoness from Marine-Derived Microorganisms: Isolation, Structure Elucidation and Biological Activities. In *Encyclopedia of Analytical Chemistry Applications, Theory and Instrumentation* (pp. 1-21).
- Pinto, M. M. M., Palmeira, A., Fernandes, C., Resende, D. I. S. P., Sousa, E., Cidade, H., Tiritan, M. E., Correia-Da-Silva, M., & Cravo, S. (2021). From Natural Products to New Synthetic Small Molecules: A Journey through the World of Xanthoness. *Molecules*, 26(2), 431.
- Pinto, M. M. M., Sousa, M. E., & Nascimento, M. S. J. (2005). Xanthone Derivatives: New Insights in Biological Activities. *Curr. Med. Chem.*, 12, 2517-2538.
- Ribero, J., Veloso, C., Fernandes, C., Tiritan, M. E., & Pinto, M. M. M. (2019). Carboxyxanthoness: Bioactive Agents and Molecular Scaffold for Synthesis of Analogues and Derivatives. *Molecules*, 24.
- Rouzer, C. A., & Marnett, L. J. (2009). Cyclooxygenases: structural and functional insights. *J. Lipid Res.*, 50(Supplement), S29-S34.
- Sathyadevi, P., Chen, Y.-J., Wu, S.-C., Chen, Y.-H., & Wang, Y.-M. (2015). Reaction-based epoxide fluorescent probe for in vivo visualization of hydrogen sulfide. *Biosensors and Bioelectronics*, 68, 681-687.
- Shao, C., Wang, C., Wei, M., Gu, Y., Xia, X., She, Z., & Lin, Y. (2008). Structure elucidation of two new xanthone derivatives from the marine fungus *Penicillium* sp. (ZZF 32#) from the South China Sea. *Magn. Reson. Chem.*, 46(11), 1066-1069.
- Shen, B. (2015). A New Golden Age of Natural Products Drug Discovery. *Cell*, 163(6), 1297-1300.
- Smith, W. L., Dewitt, D. L., & Garavito, R. M. (2000). Cyclooxygenases: Structural, Cellular, and Molecular Biology. *Annual Review of Biochemistry*, 69(1), 145-182.
- Snelgrove, P. (2016). An Ocean of Discovery: Biodiversity Beyond the Census of Marine Life. *Planta Med.*, 82(09/10), 790-799.

- Sousa, M. E. S., & Pinto, M. M. M. (2005). Synthesis of Xanthenes: An Overview. *Curr. Med. Chem.*, 12, 2447-2479.
- Sperotto, E., Van Klink, G. P. M., Van Koten, G., & De Vries, J. G. (2010). The mechanism of the modified Ullmann reaction. *Dalton Transactions*, 39(43), 10338.
- Sun, R.-R., Miao, F.-P., Zhang, J., Wang, G., Yin, X.-L., & Ji, N.-Y. (2013). Three new xanthone derivatives from an algicolous isolate of *Aspergillus wentii*. *Magn. Reson. Chem.*, 51(1), 65-68.
- Takashima, I., Kawagoe, R., Hamachi, I., & Ojida, A. (2015). Development of an AND Logic-Gate-Type Fluorescent Probe for Ratiometric Imaging of Autolysosome in Cell Autophagy. *Chemistry - A European Journal*, 21(5), 2038-2044.
- van Ryn, J., Trummelitz, G., & Pairet, M. (2000). COX-2 selectivity and inflammatory processes. *Curr. Med. Chem.*, 7(11), 1145-1161.
- Vane, J. R., & Botting, R. M. (1998). Mechanism of action of anti-inflammatory drugs: an overview. In J. Vane & J. Botting (Eds.), *Selective COX-2 Inhibitors: Pharmacology, Clinical Effects and Therapeutic Potential* 1-17.
- Vollhardt, K. P. C., & Schore, N. E. (2003). *Organic chemistry : structure and function* (4th ed. ed.). W.H. Freeman and Co.
- Yalçinyuva, T., Deligöz, H., Boz, İ., & Ali Gürkaynak, M. (2008). Kinetics and mechanism of myristic acid and isopropyl alcohol esterification reaction with homogeneous and heterogeneous catalysts. *Int. J. Chem. Kinet.*, 40(3), 136-144.
- Żelaszczyk, D., Lipkowska, A., Szkaradek, N., Słoczyńska, K., Gunia-Krzyżak, A., Librowski, T., & Marona, H. (2018). Synthesis and preliminary anti-inflammatory evaluation of xanthone derivatives. *Heterocycl. Commun.*, 24(4), 231-236.
- Zhao, Y., Wang, X., Kaneyama, R., Kodama, K., & Hirose, T. (2020). Efficient Pyrazole Moiety-Containing Ligands for Cu-Catalyzed O-Arylation of Phenols. *ChemistrySelect*, 5(14), 4152-4159.